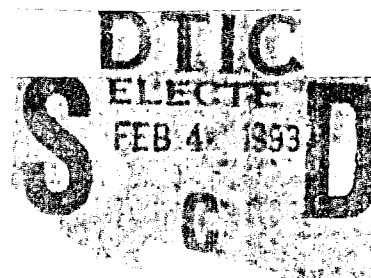


AD-A259 802



Revised  
Date: 10/10/92  
Defence  
nationalis



**EFFECT OF CODE AUGMENTATION OR  
TRUNCATION ON THE SIGNALS PRODUCED  
BY A TIME-INTEGRATING CORRELATOR**

by

**N. Brousseau**

**DEFENCE RESEARCH ESTABLISHMENT OTTAWA**  
TECHNICAL NOTE 92-11

Canada

October 1992  
Ottawa

93-01886

93 1 2 1 104



National  
Defence

Défense  
nationale

Accession For	
NTIS	<input checked="" type="checkbox"/>
DTIC TAB	<input type="checkbox"/>
Unannounced	<input type="checkbox"/>
Justification	
By	
Distribution/	
Availability Codes	
Dist	Avail and/or Special
A-1	

DTIC QUALITY INSPECTED 3

# **EFFECT OF CODE AUGMENTATION OR TRUNCATION ON THE SIGNALS PRODUCED BY A TIME-INTEGRATING CORRELATOR**

by

**N. Brousseau**

*Communications Electronic Warfare Section  
Electronic Warfare Division*

**DEFENCE RESEARCH ESTABLISHMENT OTTAWA**  
TECHNICAL NOTE 92-11

PCN  
041LQ11

October 1992  
Ottawa

## ABSTRACT

The purpose of this study is to analyse the characteristics of the signals produced by a time-integrating correlator when processing augmented or truncated codes. It deals specifically with the description of the peak trains generated by either the autocorrelation of the modified code, the cross-correlation of the modified code with the original code or the cross-correlation of the modified code with a test code of the same length. It is demonstrated that the complex peak patterns thus generated contain information about the modification of the code and that it is possible to retrieve that information by applying specific processing methods. Four processing methods are proposed. The first method extracts information from the peak patterns generated by the autocorrelation of the modified signal. The second method uses the cross-correlation of the modified signal with the original signal while the third method deals with the cross-correlation of the modified code with a test code that has the same length as the modified code. The fourth method allows the determination of the initial fill of truncated codes when the signal-to-noise ratio is sufficiently good.

## RÉSUMÉ

Le but de cette étude est d'analyser les caractéristiques des signaux produits par un corrélateur à intégration temporelle lors du traitement de codes augmentés ou tronqués. On y décrit des trains de pics produits par l'autocorrélation du code modifié, l'intercorrélation du code modifié avec le code original ou l'intercorrélation du code modifié avec un code-test de la même longueur que le code modifié. On démontre que les patrons de pics, parfois fort complexes, ainsi générés, contiennent de l'information sur la modification du code et qu'il est possible d'extraire cette information par l'application de méthodes de traitement appropriées. Quatre méthodes de traitement sont proposées. La première méthode extrait l'information des patrons de pics générés par l'autocorrélation du code modifié. La deuxième méthode utilise l'intercorrélation du signal modifié avec le signal original alors que la troisième méthode exploite l'intercorrélation du signal modifié avec un code-test qui a la même longueur que le code modifié. La quatrième méthode permet de déterminer le point de départ du code tronqué lorsque le rapport signal sur bruit est suffisamment bon.

## EXECUTIVE SUMMARY

This study demonstrates that the complex peak patterns generated by the correlation of truncated or augmented codes contains information about the modification of the code and that it is possible to retrieve that information by applying specific processing methods. Four processing methods are proposed. The first method extracts information from the peak patterns generated by the autocorrelation of the modified signal. The second method uses the cross-correlation of the modified signal with the original signal while the third method deals with the cross-correlation of the modified code with a test code that has the same length as the modified code. The fourth method allows the determination of the initial fill of truncated codes when the signal-to-noise ratio is sufficiently good.

# TABLE OF CONTENTS

	<u>PAGE</u>
ABSTRACT/RESUME	iii
EXECUTIVE SUMMARY	v
TABLE OF CONTENTS	vii
LIST OF FIGURES	ix
LIST OF TABLES	xiii
1.0 INTRODUCTION	1
2.0 FORMAT OF THE FIGURES	1
3.0 CODE AUGMENTATION	6
3.1 Autocorrelation	6
3.1.1 No data	6
3.1.2 With data	7
3.2 Cross-Correlation with the Original Code	10
3.2.1 With the same initial fill	11
3.2.2 With different initial fills	14
3.3 Cross-Correlation with a Test Code	17
3.3.1 With the same initial fill	17
3.3.2 With different initial fills	18
3.4 Determination of the Characteristics of the Augmentation	21
3.4.1 Length of the augmentation segment	21
3.4.2 Initial fill determination	22
4.0 FIRST TYPE OF CODE TRUNCATION	22
4.1 Autocorrelation	22
4.2 Cross-Correlation with the Original Code	26
4.2.1 With the same initial fill	26
4.2.2 With different initial fills	29
4.3 Cross-Correlation with a Test Code	30
4.3.1 With the same initial fill	30
4.3.2 With different initial fills	33

## TABLE OF CONTENTS (cont'd)

	<u>PAGE</u>
4.4    Determination of the Characteristics of the Truncation	36
4.4.1    Length of the truncated segment	36
4.4.2    Initial fill determination	37
5.0    SECOND TYPE OF CODE TRUNCATION	38
5.1    Autocorrelation	38
5.2    Cross-Correlation with the Original Code	45
5.2.1    With the same initial fill	45
5.2.2    With different initial fills	49
5.3    Cross-Correlation with a Test Code	55
5.3.1    With the same initial fill	55
5.3.2    With different initial fills	55
5.4    Determination of the Characteristics of the Truncation	61
5.4.1    Length of the truncated segment	61
5.4.2    Initial fill determination	62
6.0    CONCLUSION	63
6.1    First Method:    Autocorrelation of the Modified Code	63
6.1.1    No data	63
6.1.2    With data	64
6.2    Second Method:    Cross-Correlation with the Original Code	64
6.3    Third Method:    Cross-Correlation with a Test Code	64
6.4    Fourth Method:    Determination of the Initial Fill	65
6.4.1    For an augmented code	65
6.4.2    For a truncated code of the first type	65
6.4.3    For a truncated code of the second type	65
7.0    ACKNOWLEDGEMENT	65
8.0    REFERENCES	66

## LIST OF FIGURES

	<u>PAGE</u>
Figure 1: Autocorrelation of an augmented code, with no data, for $P=6$ and $p=2$ .	2
Figure 2: Chronology of peak formation for the autocorrelation of an augmented code, with no data, for $P=6$ and $p=2$ .	5
Figure 3: Autocorrelation of an augmented code, with data, for $P=6$ and $p=2$ . The data has a length of 2.	8
Figure 4: Chronology of peak formation for the autocorrelation of an augmented code, with data, for $P=6$ and $p=2$ . The data has a length of 2.	9
Figure 5: Cross-correlation of an augmented code with the original code, with no data, for $P=6$ and $p=2$ . Both the augmented code and the original code have the same initial fill.	12
Figure 6: Chronology of peak formation for the cross correlation of an augmented code with the original code, with no data, for $P=6$ and $p=2$ . Both the augmented code and the original code have the same initial fill.	13
Figure 7: Cross-correlation of an augmented code with the original code, with no data, for $P=7$ , $p=2$ , $D=4$ and $d=3$ . The augmented code and the original code have different initial fills.	15
Figure 8: Chronology of peak formation for the cross-correlation of an augmented code with the original code, with no data, for $P=7$ , $p=2$ , $D=4$ and $d=3$ . The augmented code and the original code have different initial fills.	16
Figure 9: Cross-correlation of an augmented code with a test code made up of the original code concatenated with an arbitrary segment of the same length as the augmentation, with no data, for $P=6$ , $p=2$ , $D=5$ and $d=1$ . The augmented code and the test code have different initial fills.	19

# LIST OF FIGURES (cont'd)

## PAGE

Figure 10: Chronology of peak formation for the cross-correlation of an augmented code with a test code, with no data, for $P=6$ , $p=2$ , $D=5$ and $d=1$ . The augmented code and the test code have different initial fills.	20
Figure 11: Two types of code truncation a) First type of truncation. b) Second type of truncation.	23
Figure 12: Autocorrelation of a code with the first type of truncation, with no data, for $P=6$ , $D=4$ and $d=2$ .	24
Figure 13: Chronology of peak formation for the autocorrelation of a code with the first type of truncation, with no data, for $P=6$ , $D=4$ and $d=2$ .	25
Figure 14: Cross-correlation of a code with the first type of truncation with the original code, with no data, for $P=8$ , $D=6$ and $d=2$ . The truncated code and the original code have the same initial fill.	27
Figure 15: Chronology of peak formation for the cross-correlation of a code with the first type of truncation with the original code, with no data, for $P=8$ , $D=6$ and $d=2$ . The truncated code and the original code have the same initial fill.	28
Figure 16: Cross-correlation of a code with the first type of truncation with the original code, with no data, for $P=9$ , $p=6$ , $D=2$ and $d=1$ . The truncated code and the original code have different initial fills.	31
Figure 17: Chronology of peak formation for the cross-correlation of a code with the first type of truncation with the original code, with no data, for $P=9$ , $p=6$ , $D=2$ and $d=1$ . The truncated code and the original code have different initial fills.	32



# LIST OF FIGURES (cont'd)

	<u>PAGE</u>
Figure 18: Cross-correlation of a code with the first type of truncation with a test code, with no data, for $P=4$ and $p=1$ . The test code and the truncated code have different initial fills.	34
Figure 19: Chronology of peak formation for the cross-correlation of a code with the first type of truncation with a test code of the same length, with no data, for $P=4$ and $p=1$ . The test code and the truncated code have different initial fills.	35
Figure 20: Autocorrelation of a code with a truncation of the second type, with no data, for $P=6$ , $D=4$ and $d=2$ .	39
Figure 21: Chronology of peak formation for the autocorrelation of a code with a truncation of the second type with the original code, with no data, for $P=6$ , $D=4$ and $d=2$ .	42
Figure 22: Cross-correlation of a code with a truncation of the second type with the original code, with no data, for $P=4$ , $D=3$ and $d=1$ . Both the truncated code and the original code have the same initial fill.	46
Figure 23: Chronology of peak formation for the cross-correlation of a code with a truncation of the second type with the original code, with no data, for $P=4$ , $D=3$ and $d=1$ . The truncated code and the original code have the same initial fill.	48
Figure 24: Cross-correlation of a code with a truncation of the second type with the original code, with no data, for $P=8$ , $D=5$ , $p=6$ , $d=2$ and $k=1$ . Both the truncated code and the original code have different initial fills.	50
Figure 25: Chronology of peak formation for the cross-correlation of a code with a truncation of the second type with the original code, with no data, for $P=8$ , $D=5$ , $p=6$ , $d=2$ and $k=1$ . The truncated code and the original code have different initial fills.	52

LIST OF FIGURES (cont'd)

	<u>PAGE</u>
Figure 26: Cross-correlation of a code with a truncation of the second type with a test code, with no data, for $P=8$ , $D=3$ , $p=3$ , $d=2$ and $k=1$ . Both the truncated code and the original code have different initial fills.	57
Figure 27: Chronology of peak formation for the cross-correlation of a code with a truncation of the second type with the original code, with no data, for $P=8$ , $D=3$ , $p=3$ , $d=2$ and $k=1$ . The truncated code and the original code have different initial fills.	59

# LIST OF TABLES

	<u>PAGE</u>
TABLE 1: Parameters of the peak formation process of Figures 1, 2, 3 and 4 with $P=6$ and $p=2$ .	6
TABLE 2: Parameters of the peak formation process of Figures 5 and 6 with $P=6$ and $p=2$ .	14
TABLE 3: Parameters of the peak formation process of Figures 7 and 8 with $P=7$ , $p=2$ , $D=4$ and $d=3$ .	17
TABLE 4: Parameters of the peak formation process of Figures 9 and 10 with $P=6$ , $p=2$ , $D=5$ and $d=1$ .	18
TABLE 5: Parameters of the peak formation process of Figures 12 and 13 with $P=6$ , $D=4$ and $d=2$ .	26
TABLE 6: Parameters of the peak formation process of Figures 14 and 15 with $P=8$ , $D=6$ and $d=2$ .	29
TABLE 7: Parameters of the peak formation process of Figures 16 and 17 with $P=9$ , $p=6$ , $D=2$ and $d=1$ .	33
TABLE 8: Parameters of the peak formation process of Figures 18 and 19 with $P=4$ and $p=1$ .	36
TABLE 9: Parameters of the peak formation process of Figures 20 and 21 with $P=6$ , $D=4$ and $d=2$ .	44
TABLE 10: Parameters of the peak formation process of Figures 22 and 23 with $P=4$ , $D=3$ and $d=1$ .	49
TABLE 11: Parameters of the peak formation process of Figures 24 and 25 with $P=8$ , $D=5$ , $p=6$ , $d=2$ and $k=1$ .	54
TABLE 12: Parameters of the peak formation process of Figures 26 and 27 with $P=8$ , $p=3$ , $D=3$ , $d=2$ and $k=1$ .	61

## 1.0 INTRODUCTION

Time-Integrating Correlators (TICs) are analog optical computers designed to produce the correlation of two signals. They are characterized by a variable integration time  $T$  and by time-delay windows that permit the observation of the correlation peak over a large range of relative time-shifts of the input signals. The correlation is implemented by imaging two counterpropagating signals on a detector array. The many ways to build time-integrating correlators and the factors having an influence on their performance are well documented [1-15] and are not discussed here.

The purpose of this study is to analyse the characteristics of the signals produced by a TIC processing augmented or truncated codes. It is demonstrated that it is possible to undertake to reverse the process: i.e. to determine the characteristics of a modified code from the features of the observed output of the correlator. The conditions of operation that make possible the extraction of that information are determined. Augmentation and two different types of truncation will be considered.

Previous studies [16] have analysed partial autocorrelation noise of some truncated codes of a specific length. Our study deals specifically with the description of the peak trains generated by either the autocorrelation of the modified code, the cross-correlation of the modified code with the original code or the cross-correlation of the modified code with a test code of the same length. Only the main correlation peaks are considered and binary maximum-length sequences are employed.

## 2.0 FORMAT OF THE FIGURES

If it was possible to check the status of the data produced by the detector array of a TIC without actually triggering the read-out and interrupting the correlation peak build-up process, complex and time-varying peak patterns would be observed, in most cases, when modified codes are used as inputs. The peaks would be seen to appear and grow to some maximum amplitude, then stop growing and sometimes, resume growth after a period of time. Peak formation at different locations would start and end at different times in the time-delay window of the correlator.

Figures 1, 3, 5, 7, 9, 12, 14, 16, 18, 20 22, 24 and 26 of this study describe the successive formation of peaks as it would be observed if it were possible to monitor the peak formation process on the detector array during a long integration time. Cross-correlation noise has not been taken into account; only the main correlation peaks are represented. The peak trains produced by the correlation process are illustrated using the

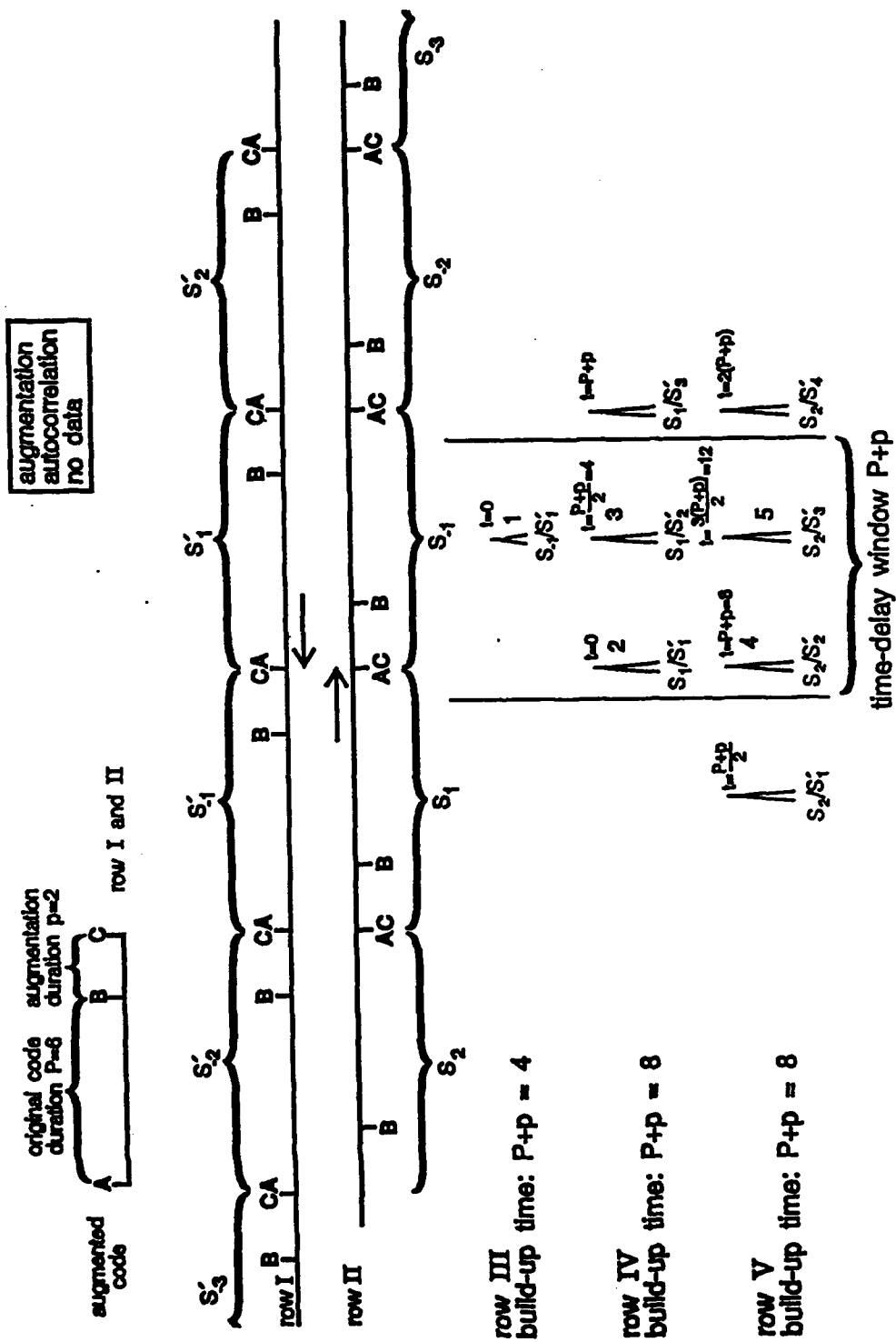


Figure 1: Autocorrelation of an augmented code, with no data, for  $P=6$  and  $p=2$ .

same format for all cases covered in this study. As a typical example, Figure 1 uses the first two rows to illustrate the relative position, at a particular time  $t=0$ , of the codes that are correlated. Various segments of the signals have been identified with letters to facilitate the discussion. The code in row I is always the modified code, augmented or truncated, and the names of its segments are denoted with a "'" such as  $S'_1$ . The code of row I is propagating from right to left at a velocity  $v$  that is a characteristic of the Bragg cells used to build the correlator. The integration by the detector array starts at  $t=0$ .

The code in row II is the other code used to perform the correlation. That code moves from the left to the right, also at a velocity  $v$ . Its various segments have also been identified with letters. For the autocorrelations, it is the same signal as in row I. For the cross-correlations it is either the original code from which the modified codes are derived, with the same or a different initial fill, or a test code of the same length as the modified code; this test code consists of the original signal, either truncated or augmented by an appropriate amount, with the same or a different initial fill. Each particular case is defined in the caption of the figures.

The signal of row III illustrates a particular train of peaks that has been formed on the detector array by the correlation of one segment of the code of row II with some of the segments of the code of row I. The two particular segments responsible for the formation of each peak are indicated below the peak. For a particular row, the peaks have been selected in such a way as to produce peaks of similar origin which require the same integration time to build. Correlation peaks are located at the meeting point of two identical counterpropagating segments in rows I and II. The time at which the formation of a particular peak begins depends on the time at which the two particular segments reach the meeting point. It is determined by the propagation time between the position of the segments at  $t=0$  and the meeting point.

All the peaks are labelled in a similar way. The starting time of the formation of the peaks is indicated at the top of each peak. The time it takes to build-up the peak of maximum amplitude is indicated at the left with the row number. The different heights associated with particular peak trains are roughly adjusted to illustrate the formation of tall or short peaks but they are not drawn to scale. A number to the right of each peak is used to identify the peak and also indicates the order of the beginning of the formation of the peak within the time-delay window indicated by a set of two vertical lines. Peaks from different types of trains are labelled with a "'" or a "" to facilitate the discussion. Tables containing the parameters of the peak formation are included for each case.

It has to be understood that although the detector array starts to integrate at  $t=0$ , most of the peaks begin formation at other times, either before or after  $t=0$ , when the signals in row I and row II become appropriately positioned. Similarly to the peaks of row III, the signals from other rows are produced by some other segments of row II correlated with many other segments of row I.

Figures 2, 4, 6, 8, 10, 13, 15, 17, 19, 21, 23, 25 and 27 illustrate the peak build-up process in the time-delay window as a function of time. Each row illustrates the peaks that would have been recorded on the detector array if the integration time had started at  $t=0$  and ended at the time associated with the row. The identification number to the right of each peak refers to the peak of the previous figure designated by the same number. For example, if a peak is designated as 1+3, it means that it is formed by the addition of the energy contained in peak number 1 and peak number 3 (see Figures 1 and 2 and Table 1). This particular method of examining the phenomenon emphasizes the evolution of the peak building process whereby peaks are generated at different locations while sometimes stopping growth for a while and then resuming growth later. The particular times which were selected to illustrate the status of the peak patterns are chosen to correspond to times when changes occur, such as the end or the beginning of the formation of a specific peak. The relative height of the peaks depends linearly on the duration of the interaction between the segments responsible for its formation, since the beginning of the integration at  $t=0$ .

The distance between the peaks in a particular train is expressed in term of time. It has the advantage of referring directly to the formation process of the peaks that is controlled by the counterpropagation at a velocity  $v$  of the two signals in the Bragg cells. If desired, distance could be calculated by multiplying the time by the velocity  $v$  of propagation of the signals in the Bragg cells.

Generally speaking, an analysis of the phenomena involved in peak formation leads to the conclusion that the observed peak pattern is the result of the interleaving of shifted peak trains. The period of the trains usually depends on the length of the modified code illustrated in row I. The shifts between the different peak trains depend on the size of the augmentation or truncation of the modified code and the amplitude of the peaks depends on the duration of the interaction between the segments generating the peaks and on the synchronization, between the integration periods and the peak formation process.

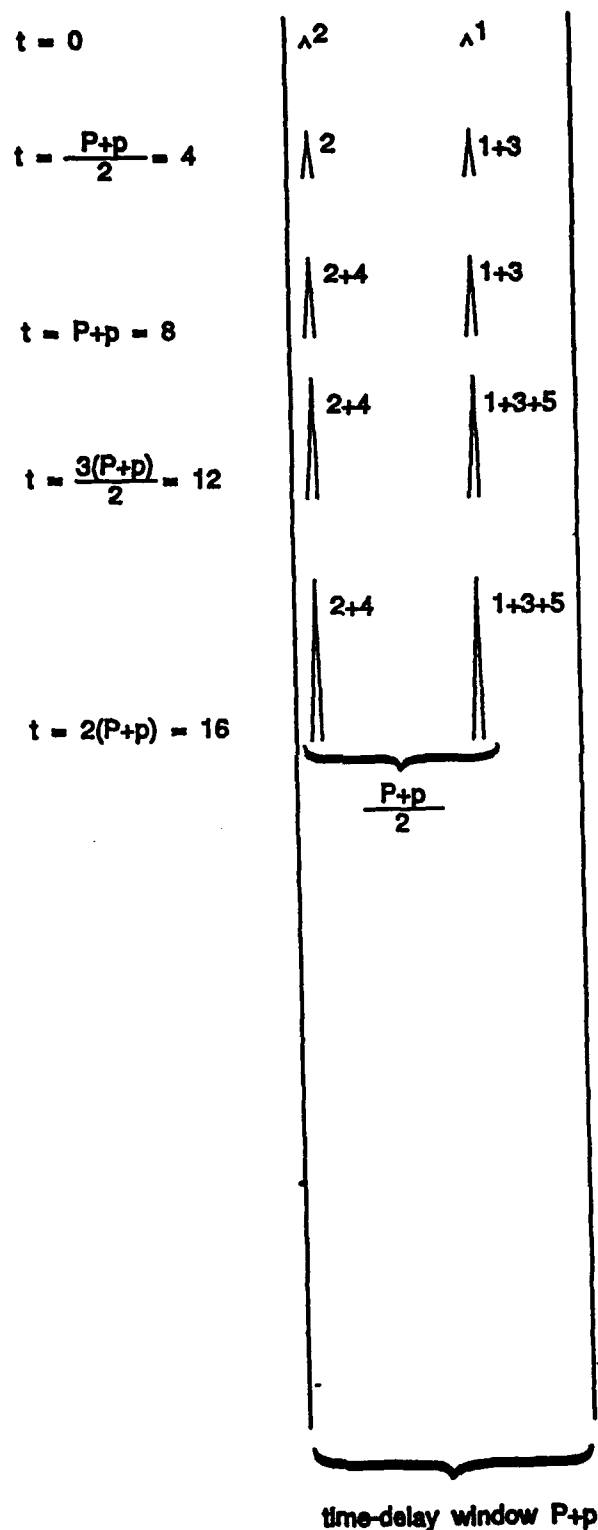


Figure 2: Chronology of peak formation for the autocorrelation of an augmented code, with no data, for  $P=6$  and  $p=2$ .



TABLE 1: Parameters of the Peak Formation Process of Figures 1, 2, 3 and 4 with  $P=6$  and  $p=2$

Peak Number	beginning of formation on the detector	duration	end of formation
1	0	$P+p=4$	$(P+p)/2=4$
2	0	$P+p=8$	$P+p=8$
3	$(P+p)/2=4$	$P+p=8$	$3(P+p)/2=12$
4	$P+p=8$	$P+p=8$	$2(P+p)=16$
5	$3(P+p)/2=12$	$P+p=8$	$5(P+p)/2=20$

### 3.0 CODE AUGMENTATION

Let us consider an original code AB with a duration  $P=6$  that is augmented by a segment BC (see Figure 1) of duration  $p=2$ . The segment BC is not a part of the segment AB. The duration of the augmented code ABC is then  $P+p=8$ . The various correlations for this augmented code will now be examined.

#### 3.1 Autocorrelation

##### 3.1.1 No Data

The autocorrelation of the augmented code is characterized by a peak train where the peaks accumulate energy continuously during the integration time. The period of the train is the length of the augmented code divided by two, that is  $(P+p)/2=4$ , and all the peaks have the same amplitude.

For example, peak #1 illustrated in row III is formed by the interaction of segment  $S_1$  and  $S_1'$  between  $t=-(P+p)/2=-4$  and  $t=(P+p)/2=4$  (see Figure 1 and Table 1). As the detector starts integrating at  $t=0$ , peak #1 will contribute energy only between  $t=0$  and  $t=(P+p)/2=4$ .

The train of peaks illustrated in row IV is formed by the correlation of the segment  $S_1$  of row II with the segments  $S_1'$ ,  $S_2'$  and  $S_3'$  of row I. The correlation peaks are separated by a distance  $(P+p)/2=4$  corresponding to half the duration of the code ABC. Similarly, the train illustrated in row V is formed by the correlation of the segment  $S_2'$  of row II with the segments  $S_1'$ ,  $S_2'$  and  $S_3'$  of row I. It is very similar to the train of row IV. The spacing and location of the peaks are the same although the peaks are not formed at the same time.

Let us now examine in Figure 2 the chronology of the events occurring in the time-delay window of duration  $P+p$  illustrated in Figure 1. The limits of the time-delay window are indicated by two vertical lines across the Figures 1 and 2. The build-up time of all peaks is  $P+p=8$ . At  $t=0$ , the segments  $S_1$  and  $S_1'$  are half way through their interaction time and start to contribute energy to a peak as soon as the detector starts to integrate. Simultaneously, peak #2 starts to build-up at  $t=0$  and stops at  $t=P+p=8$ . Peak #4 starts formation immediately thereafter, at the same location as peak #2. At  $t=(P+p)/2=4$ , peak #3 starts build-up and stops accumulating energy at  $t=3(P+p)/2=12$ . The formation of peak #5, at the same location as peak #3, starts at the moment when energy stops accumulating in peak #3. If a long integration time is used, the accumulation of energy in the various peaks will happen according to the following pattern (see Figure 2 and Table 1). Peak #2 is formed, and then, without interruption, energy continues to accumulate in peak #4 at the same location. A similar sequence of events occurs for peaks #1, #3 and #5. The final read-out from the detector array contains two peaks whose heights depends linearly on the integration time. The integration time  $T_i$  should be selected such that detectable peaks occur, taking into account the signal-to-noise ratio ( $S/N$ ) of the input.

### 3.1.2 With Data

The autocorrelation of the augmented code ABC produces a very different output when data is added to the code. The autocorrelation pattern is characterized by the presence of a single peak at the meeting point of the two codes. The peaks that could be formed at other locations are removed by successive intervals of peak build-up and decay associated with the presence of data; this tends to produce very little observable output.

The situation is illustrated in Figure 3 where the data is indicated by + and - signs at regular intervals along the code on rows I and II and, for the sake of discussion, the data duration was set to be  $(P+p)/4=2$ , one-fourth of the augmented code duration. The peak trains of rows III, IV and V are identical to the trains of Figure 1 except for one important difference. If the data is balanced, i.e. contains about the same number of + and -, then most of the peaks will have a null average amplitude; this occurs because about half of the contributions to a particular peak will be positive and the other half negative, thus cancelling each other. Those 'data destroyed' peaks are drawn with dashed lines. A positive build-up happens only at the meeting point of the two codes being autocorrelated and only one peak will be observed on the detector array.

The sequence of formation of the correlation peaks is illustrated in Figure 4 at different times that are an integer

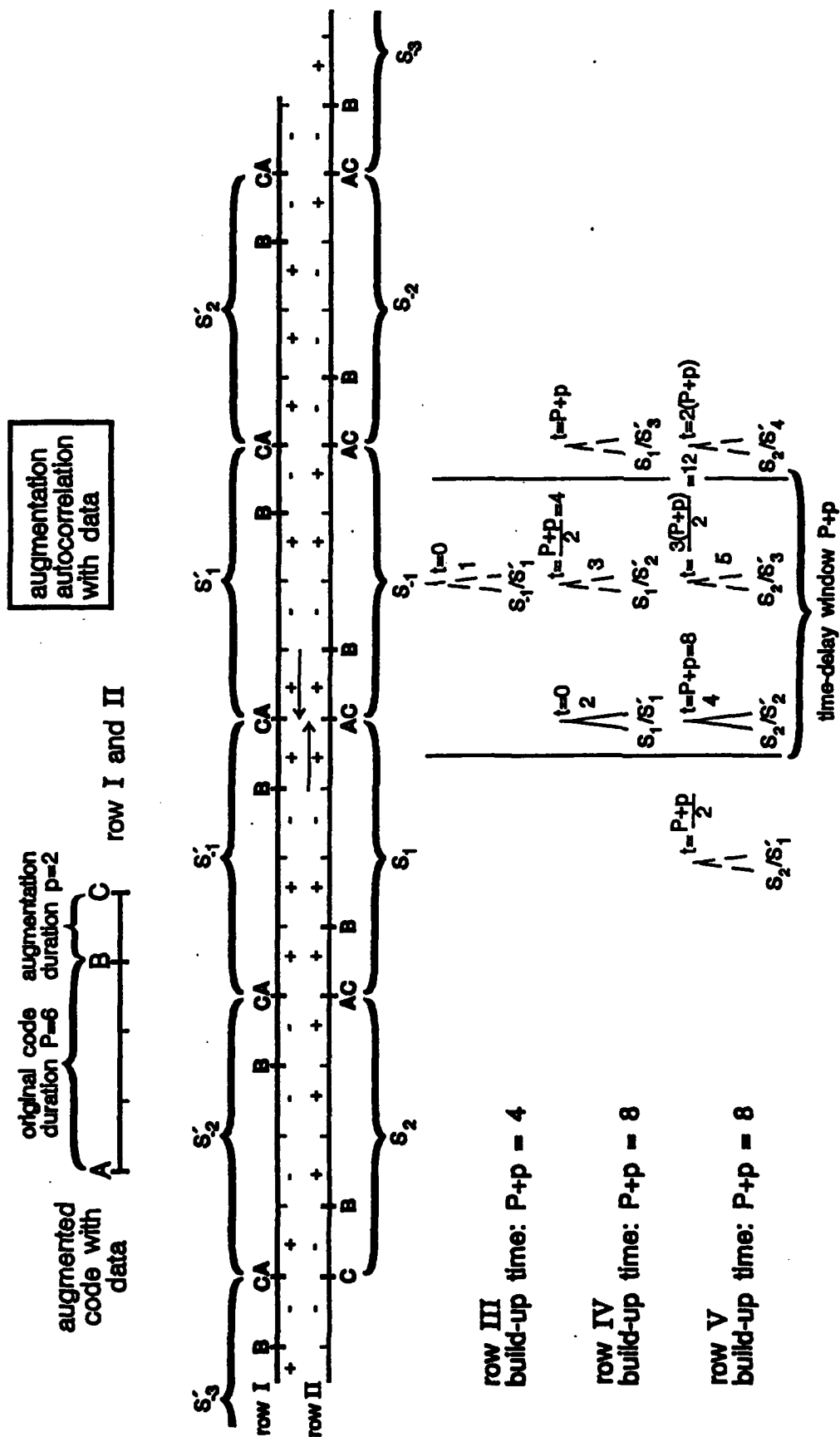


Figure 3: Autocorrelation of an augmented code, with data, for  $P=6$  and  $p=2$ . The data has a length of 2.

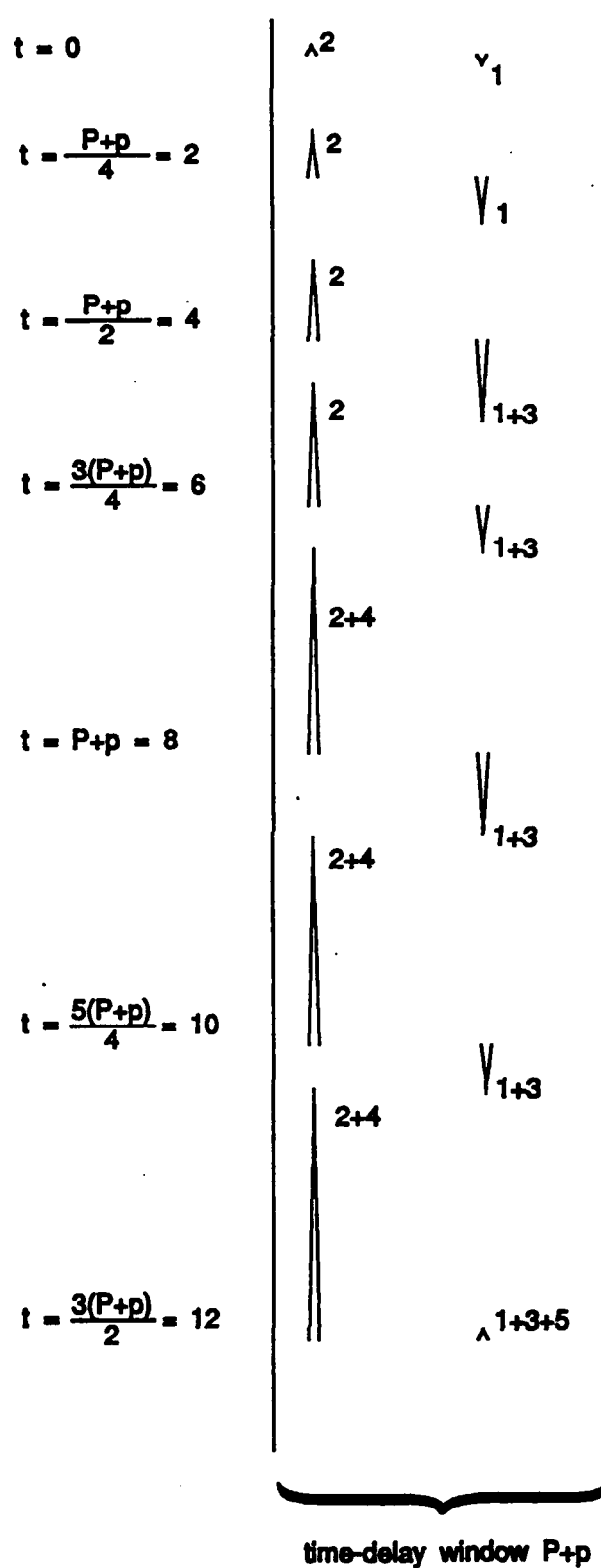


Figure 4: Chronology of peak formation for the autocorrelation of an augmented code, with data, for  $P=6$  and  $p=2$ . The data has a length of 2.

multiple of the data duration,  $(P+p)/4=2$ . The peak located to the left of the time-delay window at the meeting point of the two signals being correlated experiences a steady growth. The situation is quite different for the peaks to the right of the time-delay window that are generated first, by the correlation of  $S_1$  of row II and  $S_1'$  of row I. The accumulation of energy at that location begins when the detector array starts integrating at  $t=0$ . A negative peak is built up between  $t=0$  and  $t=(P+p)/2=4$ . Then, the positive contribution from the beginning of the interaction of the segment  $S_1$  of row II with the segment  $S_2'$  from row I, between  $t=(P+p)/2=4$  and  $t=3(P+p)/4=6$ , partially destroys the peak previously generated. Another negative contribution follows between  $t=3(P+p)/4=6$  and  $t=P+p=8$ . That contribution is destroyed by the positive contribution between  $t=P+p=8$  and  $t=3(P+p)/2=12$  and no energy is left in the peak at  $t=3(P+p)/2=12$ .

From the previous example, it can be concluded that with data present, it is difficult to draw information from the autocorrelation of the code because most of the elements of the trains of peaks are destroyed by the data. The same statement applies to the correlation of a modified code carrying data with the original code or with a test code that does not carry data.

An exception arises if the integration time necessary to produce detectable peaks is shorter than the data duration. In that case, the build-up of multiple peaks is possible because, most of the time, the integration interval does not contain a data transition. To ensure that at least one good frame containing two detectable peaks is collected, the integration time used to produce a detectable frame,  $T_i$ , has to be smaller than the time between data transitions  $D_t$  divided by two,  $T_i < D_t/2$ .

Even then, some frames will contain data transitions and the synchronization between the integration interval and the data will determine the height of the peak that will be obtained in that case. It is then a prudent practice to examine many frames to make sure that the presence of a periodic peak structure is not missed due to a data transition occurring in some of the frames.

### 3.2 Cross-Correlation with the Original Code

In this section, the cross-correlation of the augmented code with the original code is analysed for two different cases. In the first case, the original code has the same initial fill as the augmented code. In the second case, the initial fills are different.

### 3.2.1 With the Same Initial Fill

The cross-correlation of the augmented code with the original code having the same initial fill is illustrated in Figure 5 and Table 2. It is characterized by the formation of shifted peak trains where each peak benefits from a relatively short build-up time that is equal to the duration of the original code. All the peaks have the same height except for those whose formation interval includes the beginning or the end of the integration period.

Rows I and II contain repetitions of the augmented code and of the original code, respectively. Row III illustrates the train of peaks formed by the correlation of the segment  $S_1$  of row II with the segments  $S_1'$ ,  $S_2'$ ,  $S_3'$  etc. of the augmented code in row I. The peaks of row III accumulate energy during a time  $P=6$  and have a period of  $(P+p)/2=4$ . The train illustrated in row IV has been generated by the correlation of the segment  $S_2$  of row II with the segments  $S_1'$ ,  $S_2'$  and  $S_3'$  of row I. The peaks have the same build-up time and the same period as the train of row III. However, the train of row IV is shifted by an amount  $p/2=1$  relative to the train of row III. The size of the shift corresponds to the duration of the augmentation segment divided by two. The train of peaks of row V has similar properties and is characterized by a shift of  $p/2=1$  relative to the train of row IV.

Let us consider the chronology of the events that take place in the time-delay window of width  $P+p=8$  limited by the vertical lines in Figures 5 and 6. Peaks #1 and #2 of rows III and IV are first formed. Then peaks #3, #4 and #5 of rows III, IV and V, respectively, and finally, peaks #6 and #7 from rows IV and V are formed. The resulting peak pattern is made up of shifted peak trains.

The size of the augmentation can be deduced from the size of the shift between different peak trains. The longer the integration time  $T_i$ , the more trains will be formed and interleaved on the detector array. All the correlation peaks will have the same height except for those whose formation interval includes the beginning or the end of the integration. The affected peaks will not benefit from their maximum build-up time and they will have an amplitude proportional to the fraction of the build-up time within the integration time. In order to recognize the pattern of interleaved peaks, the integration time should be long enough to allow the formation of two maximum height peaks from two successive trains. The time interval between the beginning of formation of peak #1 and the end of formation of peak #4 is  $(4P+p)/2$ . We have to add another integration interval  $P$  to the total time involved in the formation of the first four peaks required to allow the formation of full height peaks. A total integration time of  $(6P+p)/2$  is required.

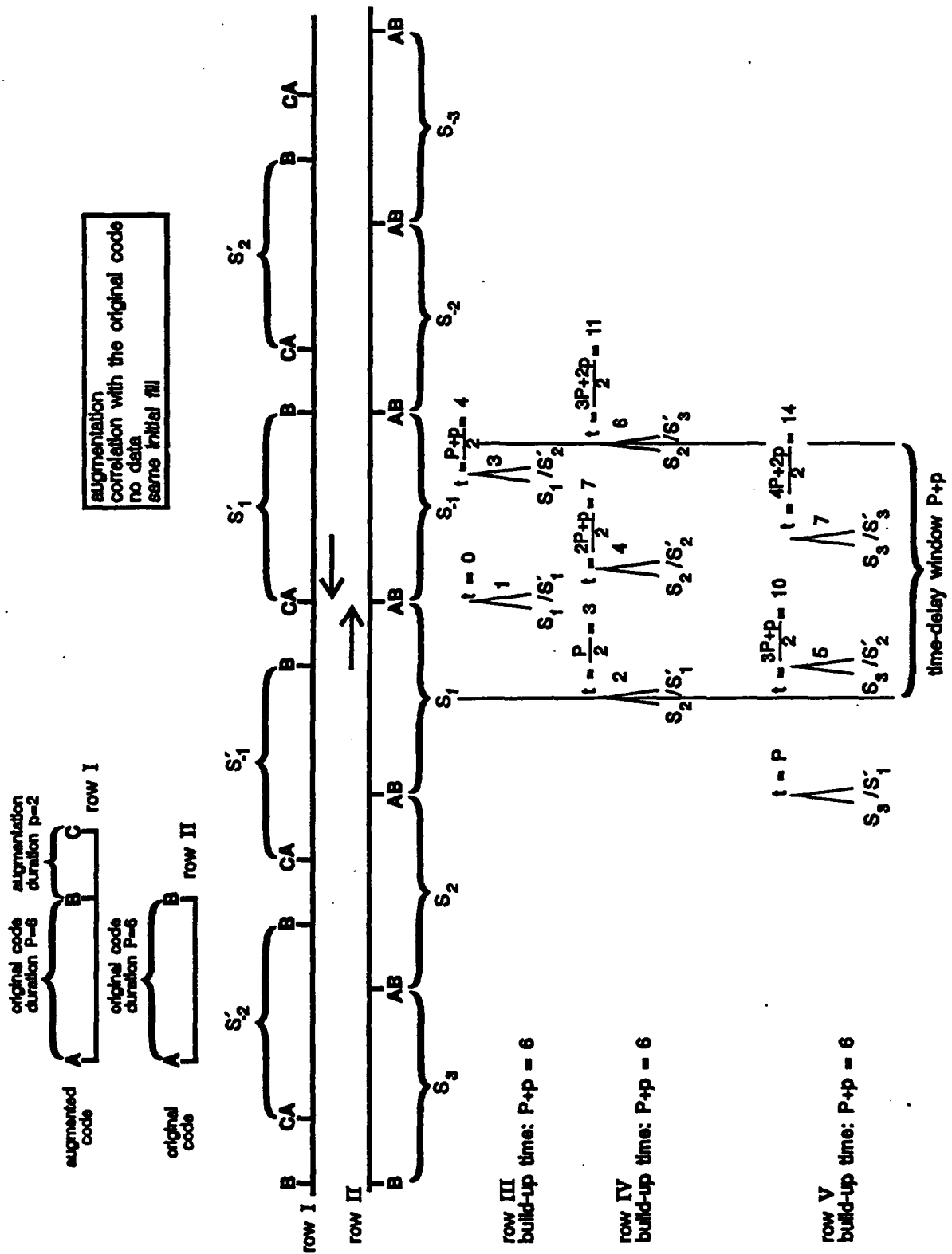


Figure 5:

Cross-correlation of an augmented code with the original code, with no data, for  $P=6$  and  $p=2$ . Both the augmented code and the original code have the same initial fill.

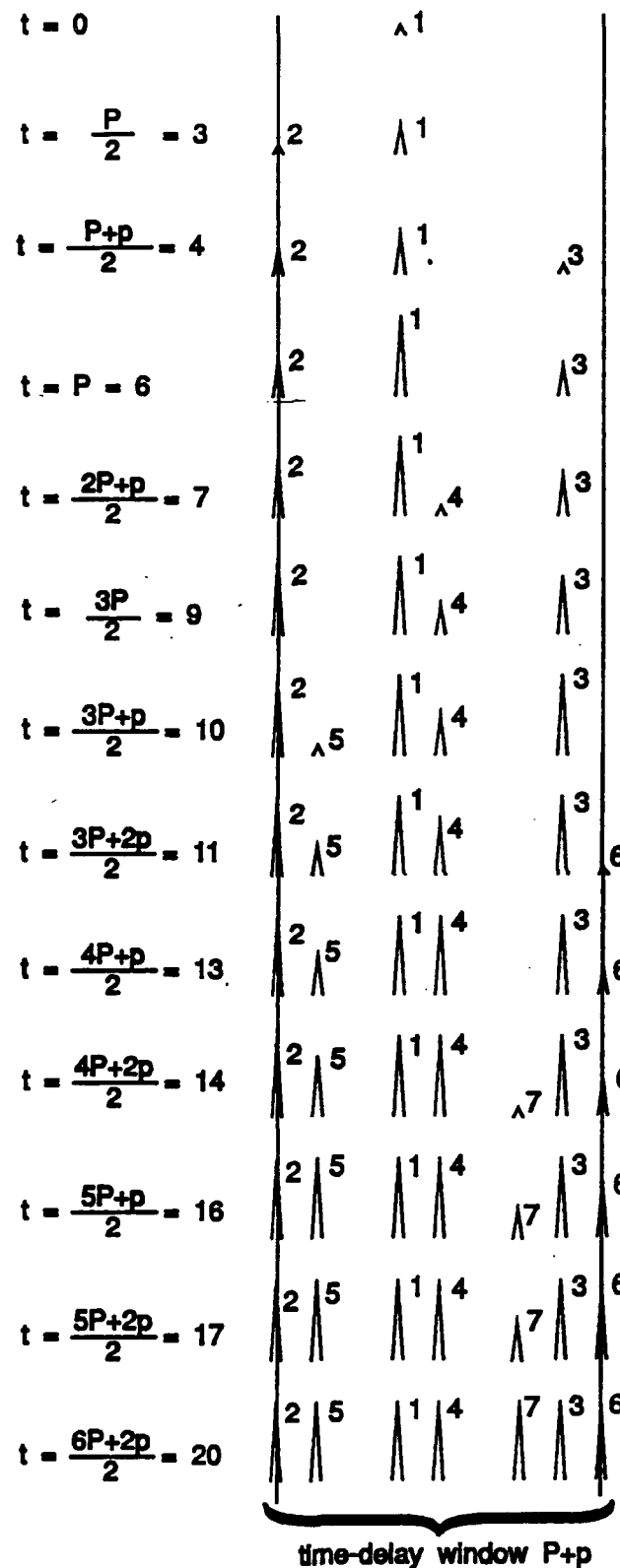


Figure 6: Chronology of peak formation for the cross-correlation of an augmented code with the original code, with no data, for  $P=6$  and  $p=2$ . Both the augmented code and the original code have the same initial fill.



TABLE 2: Parameters of the Peak Formation Process of Figures 5 and 6 with  $P=6$  and  $p=2$

Peak Number	beginning of formation on the detector	duration	end of formation
1	0	$P=6$	$P=6$
2	$P/2=3$	$P=6$	$3P/2=9$
3	$(P+p)/2=4$	$P=6$	$(3P+p)/2=10$
4	$(2P+p)/2=7$	$P=6$	$(4P+p)/2=13$
5	$(3P+2p)/2=10$	$P=6$	$(5P+p)/2=16$
6	$(3P+2p)/2=11$	$P=6$	$(5P+2p)/2=17$
7	$(4P+2p)/2=14$	$P=6$	$(6P+2p)/2=20$

However, each peak accumulates energy only during a time  $P$  and the gain produced by this integration period will set the limitation on the  $S/N$  above which it is possible to perform the analysis.

If it is desired to increase the gain by superimposing peak trains with longer integration time, random bits could be added to the original code. Using a number of bits corresponding to the augmentation length removes the drift between the trains and allows longer integration times and a correspondingly increased gain.

### 3.2.2 With Different Initial Fills

The case of the cross-correlation of an augmented code with an original code having different initial fills is particularly interesting. Trains of tall and short peaks are generated and they add up to produce an output very similar to what is obtained when the initial fills are identical.

Let us consider the sequence of events occurring in the time-delay window whose limits are indicated by the two vertical lines on Figures 7 and 8. Peak #1 appears first (see Table 3). It is formed from the cross-correlation of the segment  $S_1$  of row II with the segment  $S_1'$  of row I. Its formation starts at  $t=0$  and ends at  $t=d=3$ . On the right side of the time-delay window, peak #2 is formed from the cross-correlation of the segment  $S_1$  of row II with the segment  $S_2'$  of row I. Its formation starts at  $t=(d+p-D)/2=.5$  and ends at  $t=(d+p+D)/2=4.5$ . At the same moment that the build-up of energy stops in peak #2, it starts in peak #4. Peak #4 is at the same location as peak #2 and originates from the cross-correlation of segment  $S_1$  from row II with segment  $S_3'$  from row I. The formation of peak #4 will end at  $t=(p+2d+2D)/2=8$ . Peak #2 and peak #4 originate from segments of

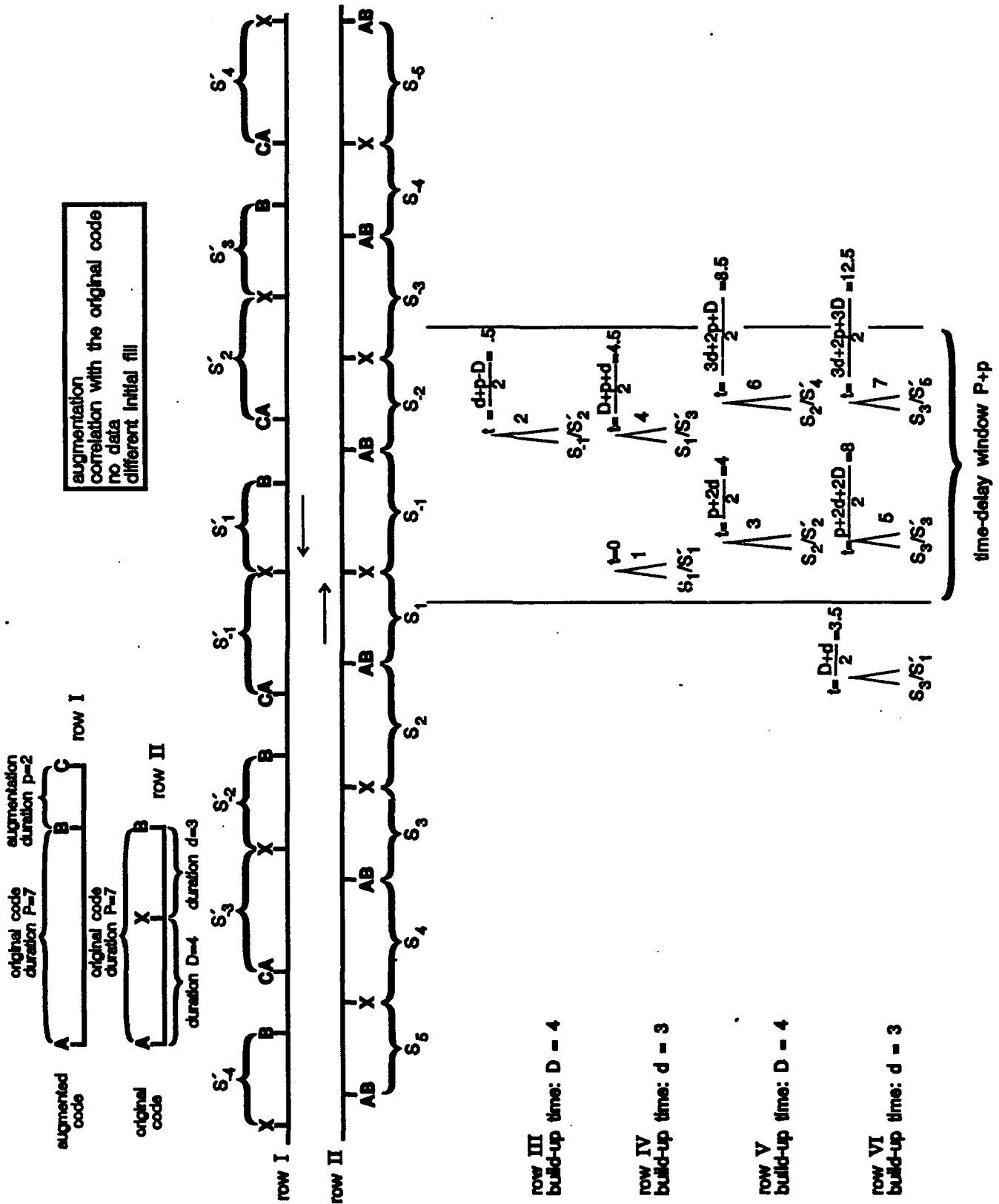


Figure 7: Cross-correlation of an augmented code with the original code, with no data, for P=7, p=2, D=4 and d=3. The augmented code and the original code have different initial fills.

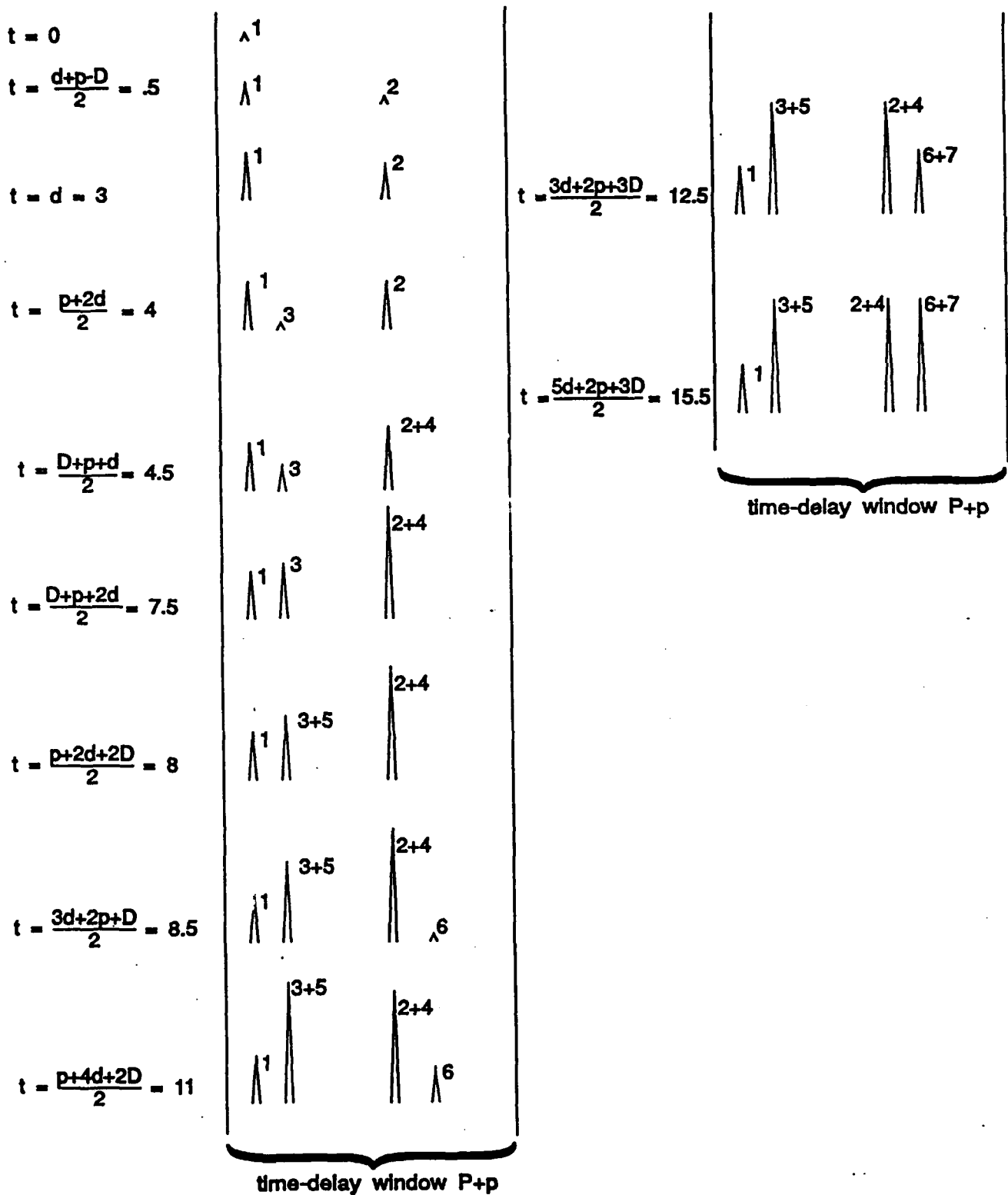


Figure 8: Chronology of peak formation for the cross-correlation of an augmented code with the original code, with no data, for  $P=7$ ,  $p=2$ ,  $D=4$  and  $d=3$ . The augmented code and the original code have different initial fills.

the original code that have been shuffled by using a different initial fill and they cannot be distinguished from each other. Similar results can be found for the peak pairs 3-5 and 6-7. In practice, the cross-correlation of an augmented code with the original code produces peak patterns that are independent of the initial fill used. The chronology of peak formation is illustrated in Figure 8 and it can be observed that the resulting signals are indistinguishable from what is obtained when the same initial fill is used. The period of the trains, in both cases, is determined by the total length of the augmented code. The shift between the trains depends on the length of the augmentation and the total build-up time is equal to the duration of the original code.

TABLE 3: Parameters of the Peak Formation Process of Figures 7 and 8 with  $P=7$ ,  $p=2$ ,  $D=4$  and  $d=3$

Peak Number	beginning of formation on the detector	duration	end of formation
1	0	$d=3$	$d=3$
2	$(d+p-D)/2=.5$	$D=4$	$(d+p+D)/2=4.5$
3	$(p+2d)/2=4$	$D=4$	$(p+2d+2D)/2=8$
4	$(D+p+d)/2=4.5$	$d=3$	$(D+p+3d)/2=7.5$
5	$(p+2d+2D)/2=8$	$d=3$	$(p+4d+2D)/2=11$
6	$(3d+2p+D)/2=8.5$	$D=4$	$(3d+2p+3D)/2=12.5$
7	$(3d+2d+3D)/2=12.5$	$d=3$	$(5d+2p+3D)/2=15.5$

The integration time  $T_i$  that allows the formation of two maximum height peaks from two successive trains and thus to recognize the pattern of interleaved peaks is  $T_i > (3d+4p+3D)/2$ .

### 3.3 Cross-Correlation with a Test Code

#### 3.3.1 With the Same Initial Fill

Let us define the test code associated with an augmented code as the code made up of the concatenation of the original code with a random sequence of bits having the same length as the augmentation. If the initial fills of the augmented code and of the test code are the same, the segments AX and XB of the test code are contiguous. Only one train of peaks is formed and the peak pattern is the same as for the autocorrelation except that the peaks are easier to detect because the test code does not contain any noise. For a given S/N of the augmented code, the integration time  $T_i$  necessary to produce detectable peaks is expected to be half of what was necessary for the autocorrelation.

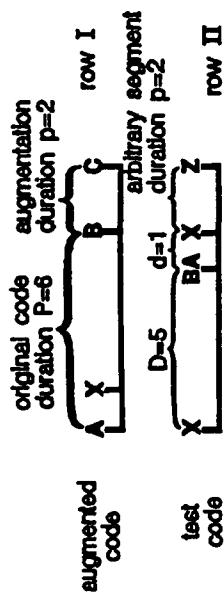
### 3.3.2 With Different Initial Fills

The properties of the cross-correlation of the augmented code with a test code made up of the original code concatenated with an arbitrary segment XZ having the same length as the augmentation but a different initial fill is particularly interesting. Figures 9 and 10 and Table 4 describe the peak formation process. Two trains of correlation peaks are formed and their relative amplitude depends on the location of the starting point of the test code relative to the starting point of the augmented code.

TABLE 4: Parameters of the Peak Formation Process of Figures 9 and 10 with  $P=6$ ,  $p=2$ ,  $D=5$  and  $d=1$

Peak Number	beginning of formation on the detector	duration	end of formation
1	0	$d=1$	$d=1$
2	$(P+p)/2=4$	$d=1$	$(P+p+2d)/2=5$
3	$P+p=8$	$d=1$	$P+p+d=9$
4	$3(P+p)/2=12$	$d=1$	$(3P+3p+2d)/2=13$
5	$(p+2d)/2=2$	$D=5$	$(p+2d+2D)/2=7$
6	$(2p+P+2d)/2=6$	$D=5$	$(2p+P+2d+2D)/2=11$
7	$(3p+2P+2d)/2=10$	$D=5$	$(3p+2P+2d+2D)/2=15$
8	$(3p+2P+2d)/2=10$	$D=5$	$(3p+2P+2d+2D)/2=15$
9	$(4p+3P+2d)/2=14$	$D=5$	$(4p+3P+2d+2D)/2=19$
10	$(5p+4P+2d)/2=18$	$D=5$	$(5p+4P+2d+2D)/2=23$

Two trains are formed because the different initial fills for the augmented code and the test code means the segments AX and XB of the test code are no longer contiguous as is the case when they have the same initial fill. The shift between the two trains of peaks is proportional to the size of the augmentation segment. In Figure 9, the short train of peaks is formed by the autocorrelation of the segment AX of both the augmented code and the test code. The tall trains of peaks formed by the cross-correlation of the segment XB of the augmented code is shifted because of the presence of the arbitrary segment XZ between the segments AX and XB of the test code.



augmentation correlation with a test code no data different initial fill

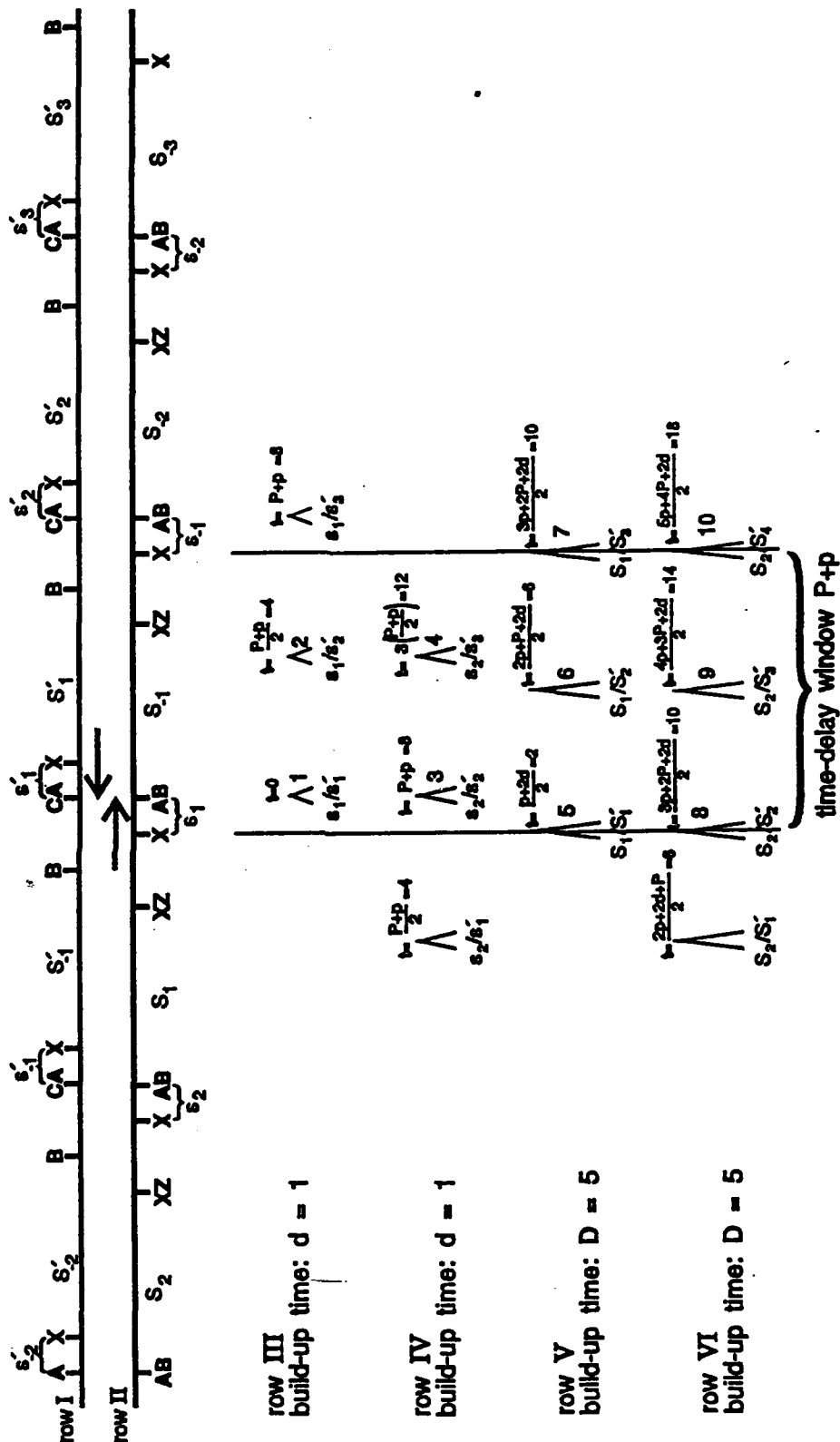


Figure 9:

Cross-correlation of an augmented code with a test code made up of the original code concatenated with an arbitrary segment of the same length as the augmentation, with no data, for  $P=6$ ,  $p=2$ ,  $D=5$  and  $d=1$ . The augmented code and the test code have different initial fills.

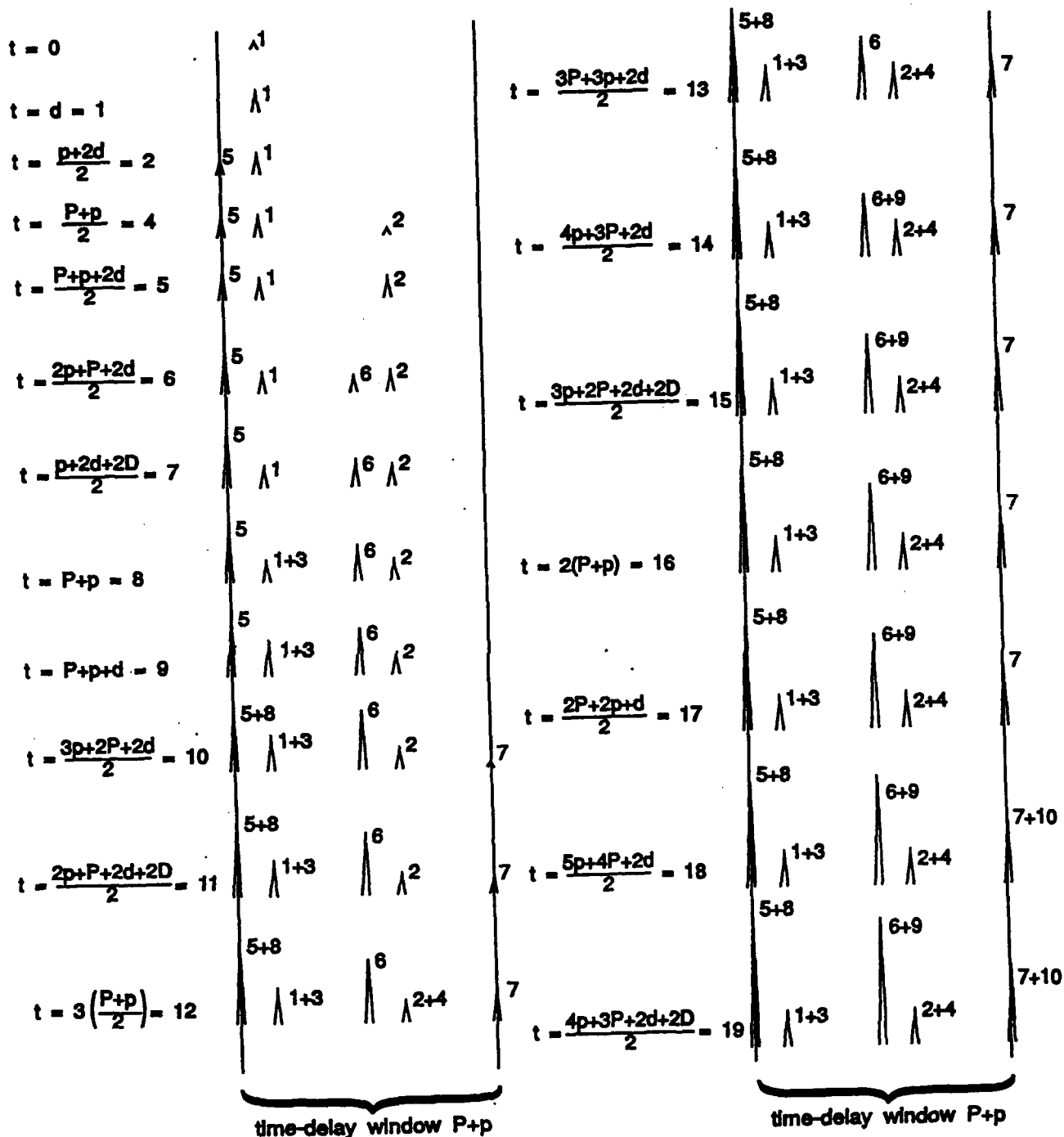


Figure 10: Chronology of peak formation for the cross-correlation of an augmented code with a test code, with no data, for  $P=6$ ,  $p=2$ ,  $D=5$  and  $d=1$ . The augmented code and the test code have different initial fills.

The integration time has to be adjusted for the worst case that occurs when the starting point X of the test code is very close to the starting point of the original code AB. Two peak trains are formed and one of the trains contains tall peaks and the other contains very small peaks. The integration time associated with the S/N of the augmented code has to be adjusted to allow, if possible, the detection of the small peaks.

### 3.4 Determination of the Characteristics of the Augmentation

The previous analysis suggests a few specific methods to extract information from the correlograms produced by augmented codes.

#### 3.4.1 Length of the Augmentation Segment

Three different methods are possible to evaluate the length of the augmentation segment. Using the first method, it is possible to determine the length of the augmentation segment from the period of the peak pattern of the autocorrelation if the signal does not contain data. The integration time should be long enough to produce sufficient gain to detect the correlation peaks and to establish the period of the peak train. The period of the peak trains can be used to calculate the discrepancies between the expected length of the maximum-length code and the observed period. If data is present, it is difficult to draw information from the autocorrelation of the code about the presence or absence of augmentation or about the length of the modification because most of the elements of the trains of peaks are destroyed by the data. The same statement applies to the correlation of a modified code carrying data with the original code or with a test code that does not carry data.

The length of the augmentation segment can also be determined, using the second method, by measuring the shift between the peak trains produced by the cross-correlation of the augmented code with the original code. An integration time of at least three times the duration of the original code allows the formation of two successive maximum height peaks from two successive interleaved trains. However, each peak will benefit from an integration time of only P and it may not be sufficient to allow the detection of the peak pattern if too much noise is present.

Using the third method, superimposed peak trains can be obtained in forming a test code by adding random bits to the original code. Using the same number of bits as the augmentation segment removes the drift between the trains and allows longer integration times and a correspondingly increased gain. If the test code has the same initial fill as the augmented code, the peak pattern is identical to the autocorrelation case except that the peaks are easier to detect because the test code does not



contain any noise. If the test code does not have the same initial fill as the augmented code, two peak trains are formed. The relative height of the two trains depends on the starting point of the code and the worst case, from a peak detection point of view, occurs when the starting point X of the test code is very close to the starting point of the original code AB. Two peak trains are formed, one containing tall peaks and the other containing very small peaks. The integration time associated with the S/N of the augmented code has to be adjusted to allow, if possible, the detection of the small peaks.

#### 3.4.2 Initial Fill Determination

If the S/N of the augmented code is very good, the cross-correlation of the augmented code with a test code could allow the determination of the initial fill. The procedure to follow is to successively try all possible initial fills. When the right fill is found, only one peak train is present in the correlation pattern.

### 4.0 FIRST TYPE OF CODE TRUNCATION

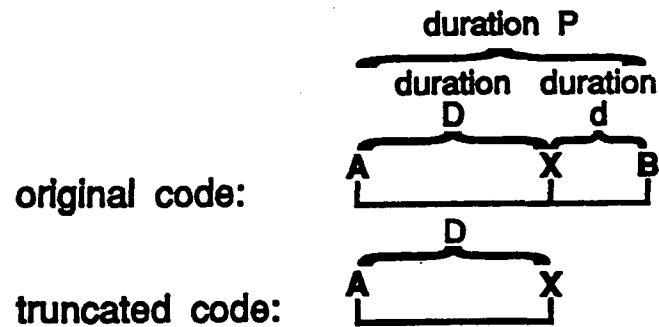
Code truncation can be performed in two different ways. The first method is illustrated in Figure 11a. A code AB with period P is truncated at a point X defining a segment AX of duration D and a segment XB of duration d. The segment XB is removed and a truncated code of period D is formed.

In the second method (see Figure 11b), the signal contains a full period AB of the code followed by a partial repeat AX of the code AB. The period of the resulting sequence ABX is  $P+D$ .

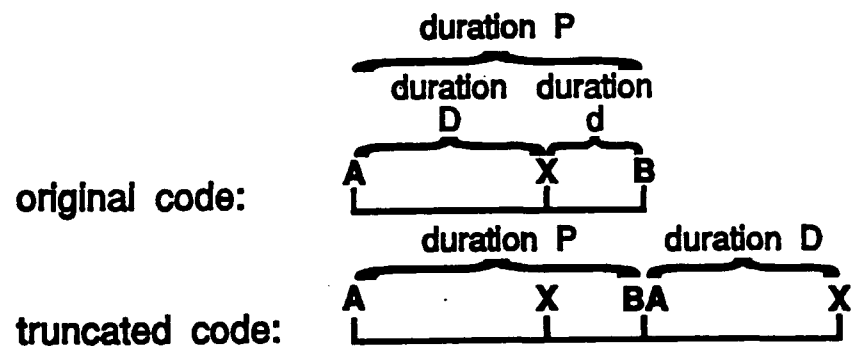
#### 4.1 Autocorrelation

Let us consider the autocorrelation of the first type of truncated code. The autocorrelation (see Figures 12 and 13 and Table 5) of the code produces aligned peak trains with a period of  $D/2$ , the duration of the truncated code divided by two. All the peaks have the same amplitude and accumulate energy continuously.

Figure 13 illustrates the chronology of the peak formation and it can be observed that the peaks grow continuously. In order to obtain enough gain to allow the determination of the period of the peaks for the S/N of the truncated code, the integration time should be sufficient to allow the detection of the peaks of the trains. The results of the analysis presented in Section 3.1.2 on the effect of the



a) First type of truncation



b) Second type of truncation

Figure 11: Two types of code truncation  
a) First type of truncation.  
b) Second type of truncation.



- 24 -

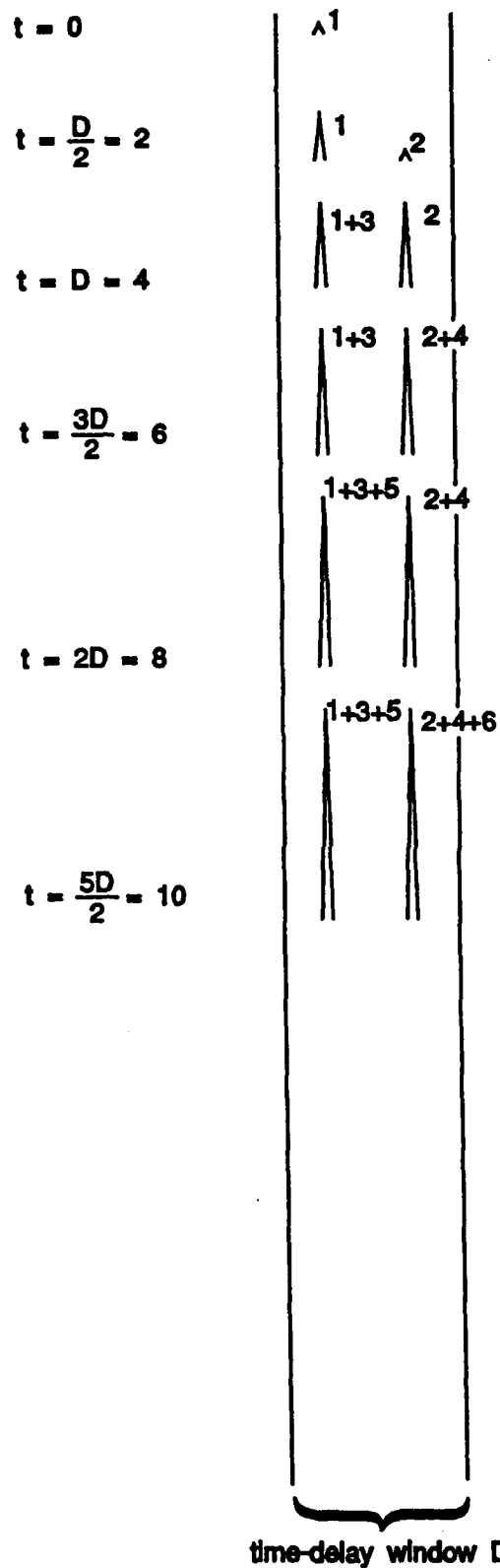


Figure 13: Chronology of peak formation for the autocorrelation of a code with the first type of truncation, with no data, for  $P=6$ ,  $D=4$  and  $d=2$ .

TABLE 5 Parameters of the Peak Formation Process of  
Figures 12 and 13 with  $P=6$ ,  $D=4$  and  $d=2$

Peak Number	beginning of formation on the detector	duration	end of formation
1	0	$D=4$	$D=4$
2	$D/2=2$	$D=4$	$3D/2=6$
3	$D=4$	$D=4$	$2D=8$
4	$3D/2=6$	$D=4$	$5D/2=10$
5	$2D=8$	$D=4$	$3D=12$
6	$5D/2=10$	$D=4$	$7D/2=14$

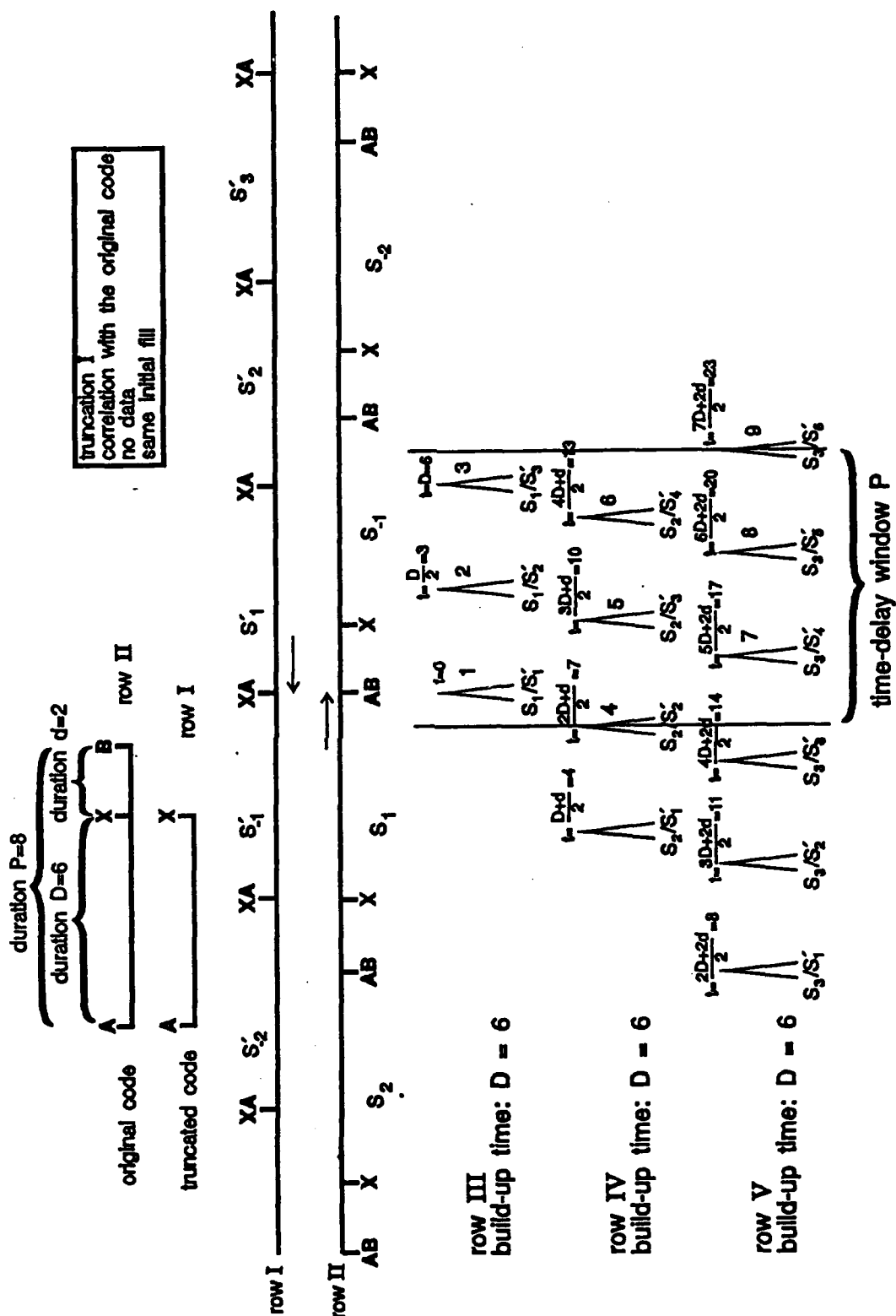
presence of data also apply to this case. Consequently, the autocorrelation will give useful results only when there is no data on the signal or if an integration time shorter than the data length divided by two can be used to produce enough gain to detect the peaks.

#### 4.2 Cross-Correlation with the Original Code

The structure of the peaks trains produced by the cross-correlation of a code having the first type of truncation with the original code is characterized by shifted peak trains of equal height having a period  $D/2$  equal to the duration of the truncated code  $D$  divided by two. The size of the shift between the trains is equal to the length of the truncated segment divided by two.

##### 4.2.1 With the same initial fill

The peak trains produced by the cross-correlation of the truncated code with the original code, when both have the same initial fill, are illustrated in Figures 14 and 15. Row III contains the peak train formed by the cross-correlation of the segment  $S_1$  of row II with the segments  $S_1'$ ,  $S_2'$ ,  $S_3'$  and  $S_4'$  of row I (see Table 6). The build-up time of each peak is  $D$  and the period of the peak train is  $d/2$ . Row IV contains the peak train formed by the cross-correlation of the segment  $S_2$  of row II with the segments  $S_1'$ ,  $S_2'$ ,  $S_3'$  and  $S_4'$  of row I. The build-up time and the period of the peak train are identical to the peak train of row III. The only difference is that the peak train of row IV is shifted by an amount  $d/2$  relative to the peak train of row III; this is equal to the length of truncation of the original code divided by two. Similar comments apply to the peak train of row V.



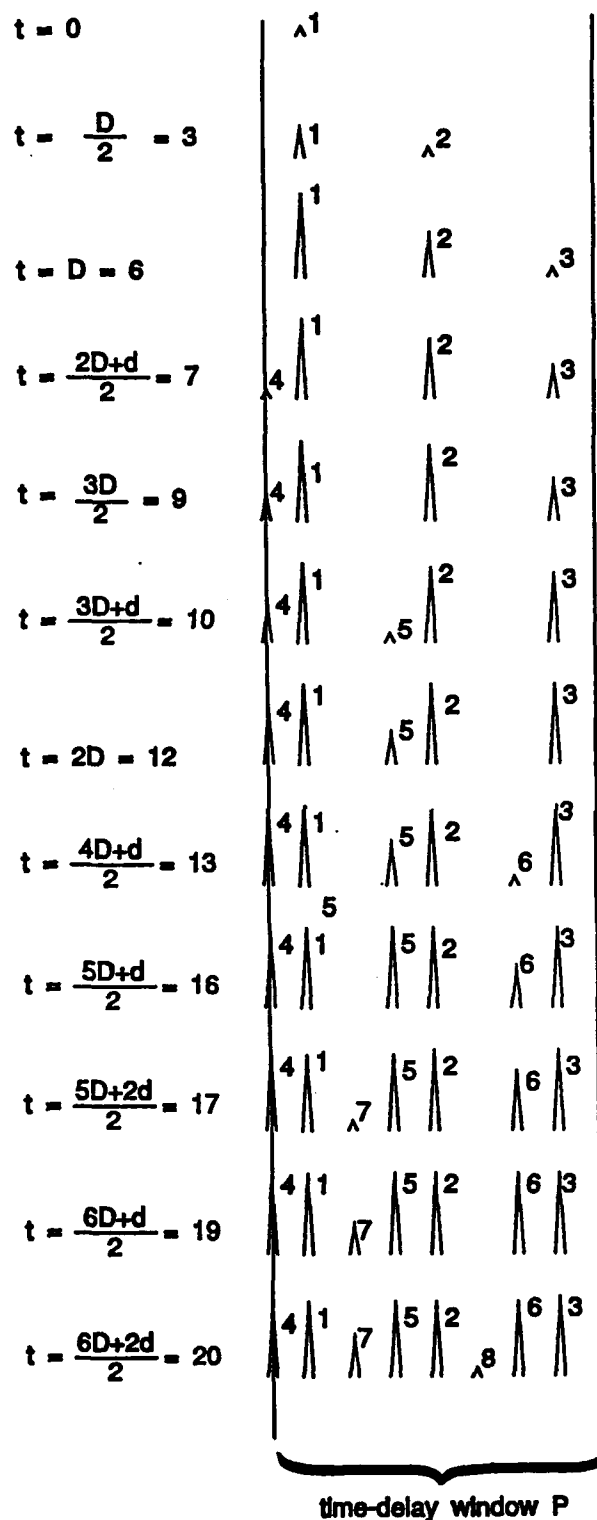


Figure 15: Chronology of peak formation for the cross-correlation of a code with the first type of truncation with the original code, with no data, for  $P=8$ ,  $D=6$  and  $d=2$ . The truncated code and the original code have the same initial fill.

TABLE 6: Parameters of the Peak Formation Process of  
Figures 14 and 15 with  $P=8$ ,  $D=6$  and  $d=2$

Peak Number	beginning of formation on the detector	duration	end of formation
1	0	$D=6$	$D=6$
2	$D/2=3$	$D=6$	$3D/2=9$
3	$D=6$	$D=6$	$2D=12$
4	$(2D+d)/2=7$	$D=6$	$(4D+d)/2=13$
5	$(3D+d)/2=10$	$D=6$	$(5D+d)/2=16$
6	$(4D+d)/2=13$	$D=6$	$(6D+d)/2=19$
7	$(5D+2d)/2=17$	$D=6$	$(7D+2d)/2=23$
8	$(6D+2d)/2=20$	$D=6$	$(8D+2d)/2=26$
9	$(7D+2d)/2=23$	$D=6$	$(9D+2d)/2=29$

The chronology of the events (see Table 6) occurring in the time-delay window of width  $P$ , whose limits are indicated by two vertical lines in Figure 14, is illustrated in Figure 15. The peak train of row III is first built, then it is followed by the peak trains of row IV and V. As time goes by, the interleaving of new peak trains complicates the situation but, after a certain time, a regular pattern of peaks tends to form. They are separated by a distance  $d/2$  where  $d$  is the duration of the segment that was removed from the original code. All of the peaks have the same build-up time and eventually reach the same height if the integration time is sufficiently long. An integration time of at least  $T_i=(5D+d)/2$  is required to produce two successive peaks from two successive shifted trains. As the peak formation process is not synchronized with the detector integration periods, increasing the integration time to  $(7D+d)/2$  allows the formation of the four peaks of interest with maximum height.

#### 4.2.2 With Different Initial Fills

The structure of the train of peaks produced by the cross-correlation of the truncated code with the original code when they have different initial fills is much simpler than for the augmented case (see section 3.2.1). The reason for that difference is that, for the case of the truncation, there are no extra bits to generate a break in the correlation process. The peaks that are generated by a long integration time are the



result of interleaving shifted trains of peaks that have the same period and the same build-up time. No train of short peaks appears. It is interesting to compare this situation with the augmented code where the augmentation segment causes an interruption in the peak formation because it does not correlate with any part of the original code. As the augmentation segment can be placed anywhere in the original code, the interruption generated by the augmentation segment produces trains of short and tall peaks (see Figure 8).

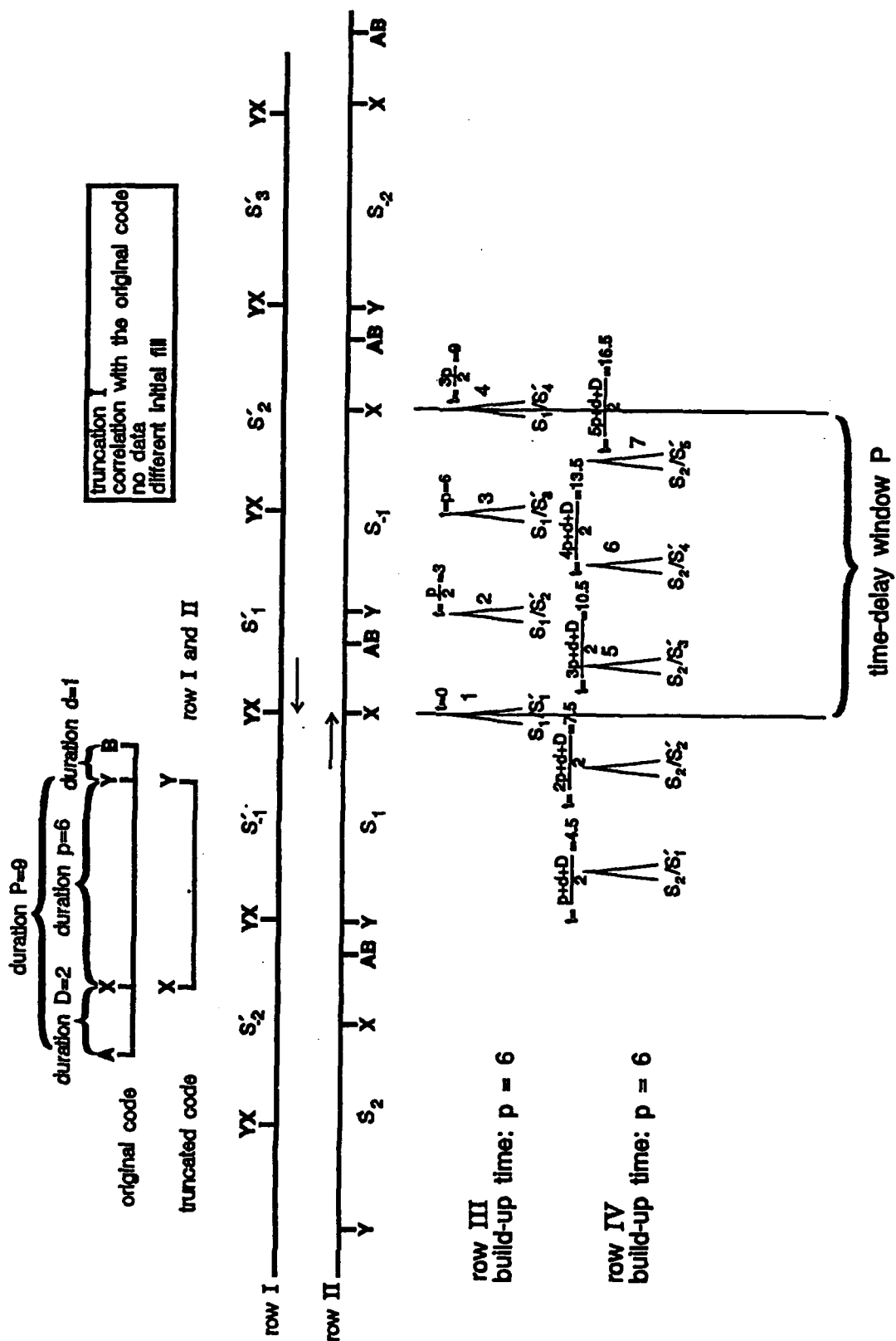
In the particular example illustrated in Figure 16, the peaks of row III are first generated (see Table 7), followed by the peaks of row IV that form a shifted peak train. The peaks have a build-up duration of  $p=6$  and a period of  $p/2$  where  $p$  is the length of the truncated code. It is possible to calculate the length of the truncation by measuring the size of the shift between different peak trains or the period of the peak trains. As in the previous case with the same initial fill, an integration time of  $(8p+d+D)/2$  is required to produce two successive full height peaks from two successive shifted peak trains. However, peak detection will be possible only if the build-up time  $p=6$  of each peak is sufficient to produce a detectable peak considering the  $S/N$  of the truncated code.

#### 4.3 Cross-Correlation with a Test Code

##### 4.3.1 With the Same Initial Fill

Let us define the test code associated with a truncated code of the first type as the code made up of the original code truncated to have the same length as the truncated code. The cross-correlation of the truncated code with a test code having the same length as the truncated code produces unshifted, equal height peak trains and it is then possible to use a longer integration time to extract correlation peaks from noisy input signals.

If the initial fills of the truncated and of the test code are the same, the test code and the truncated code are identical, except for their  $S/N$ . Similarly, the train of peaks that is formed is the same as for the autocorrelation case except that the peaks are easier to detect because the test code does not contain any noise. The integration time  $T_i$  necessary to produce detectable peaks is expected to be half of that required for the autocorrelation for a given  $S/N$  of the augmented code.



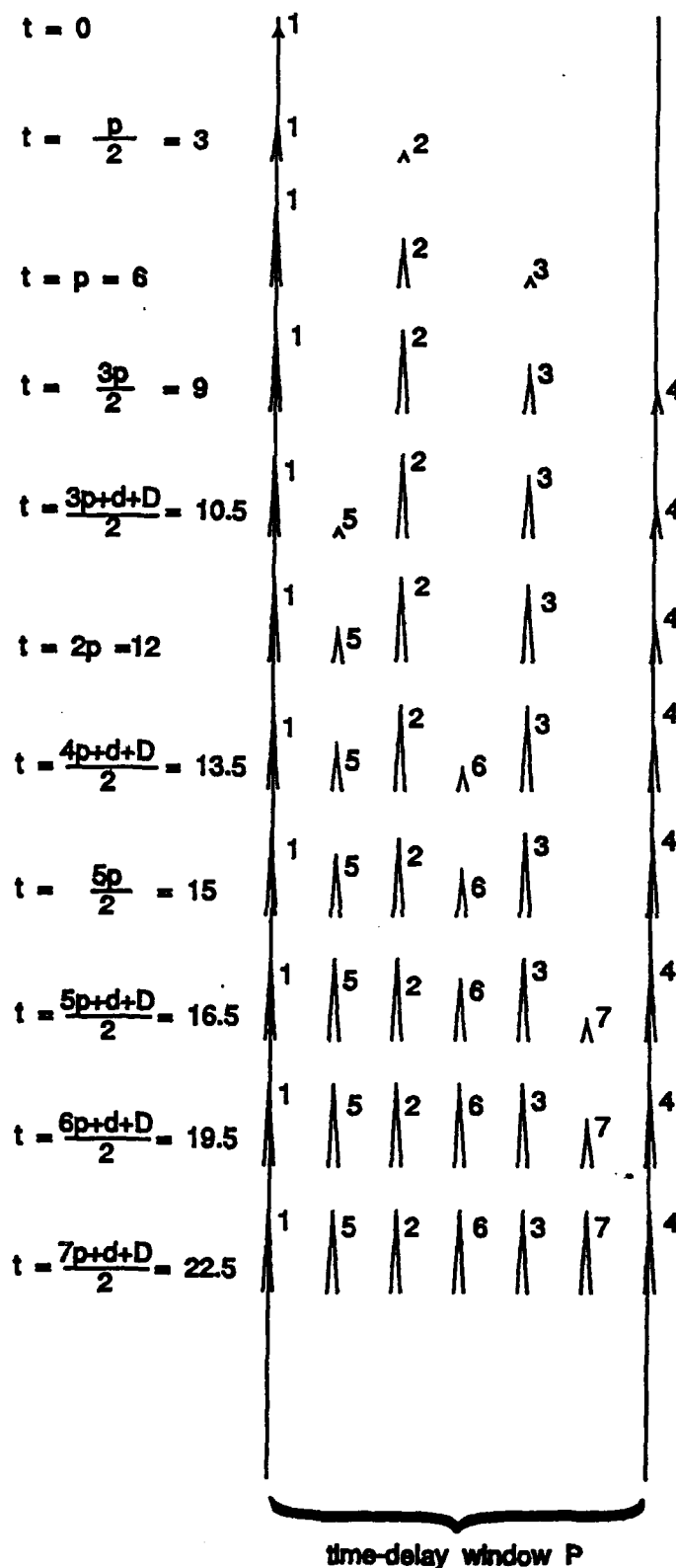


Figure 17: Chronology of peak formation for the cross-correlation of a code with the first type of truncation with the original code, with no data, for  $P=9$ ,  $p=6$ ,  $D=2$  and  $d=1$ . The truncated code and the original code have different initial fills.

TABLE 7: Parameters of the Peak Formation Process of  
Figures 16 and 17 with  $P=9$ ,  $p=6$ ,  $D=2$  and  $d=1$

Peak Number	beginning of formation on the detector	duration	end of formation
1	0	$p=6$	$p=6$
2	$p/2=3$	$p=6$	$3p/2=9$
3	$p=6$	$p=6$	$2p=12$
4	$(3p/2)=9$	$p=6$	$5p/2=15$
5	$(3p+d+D)/2=10.5$	$p=6$	$(5p+d+D)/2=16.5$
6	$(4p+d+D)/2=13.5$	$p=6$	$(6p+d+D)/2=19.5$
7	$(5p+d+D)/2=16.5$	$p=6$	$(7p+d+D)/2=22.5$

#### 4.3.2 With Different Initial Fills

Figures 18 and 19 illustrate respectively the peak formation process and the chronology of the events (see Table 8) when the two codes have different initial fills. The key feature of the peak patterns is that all the peaks have the same height. However, the peaks do not accumulate energy all the time. Periods of growth are followed by periods where no energy accumulates in the peak.

Row III of Figure 18 illustrates the formation of the first train of peaks. Peak #1 starts formation at  $t=-(p+P)=-5$  and ends it at  $t=-p=-1$ . It does not contribute to the energy accumulated at that location because the integration starts at  $t=0$ . Peak #1 has been included for the sake of completeness. Peaks #2 and #3 also belong to the same train whose period is  $(P+p)/2$ , the length of the truncated code divided by two. The next two peak trains illustrated in rows IV and V, respectively, are aligned and have the same period. The alignment of the trains produces an accumulation of energy at a few specific locations. Examining the chronology of the accumulation of energy in the middle of the time-delay window where peaks #2, #5 and #6 are produced (see Figure 19 and Table 8), it is seen that peak #2 starts and terminates its formation at  $t=-(P+p)/2=-2.5$  and  $t=(P-p)/2=1.5$ . The detector collects only the energy produced after  $t=0$ . There is then an interval  $t=p$  long during which no energy accumulates on the detector followed by the formation of peak #5. Another interval with no energy accumulation follows and finally peak #8 adds its contribution to the energy already accumulated at that location.



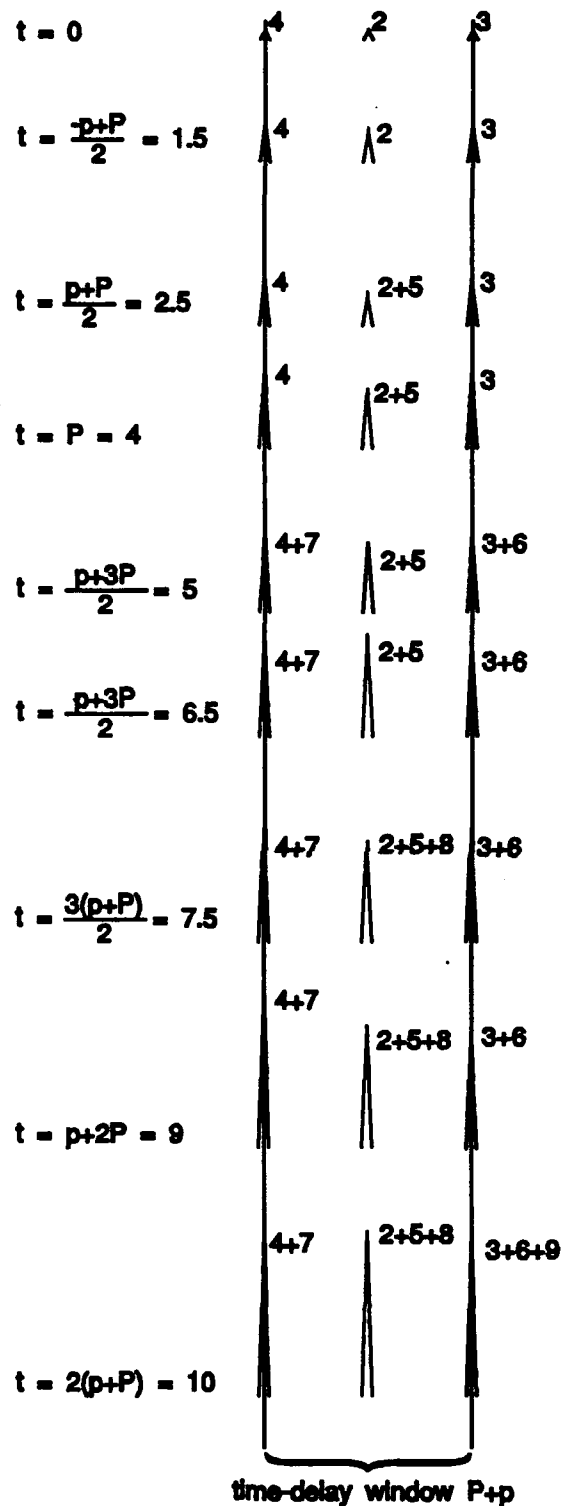


Figure 19: Chronology of peak formation for the cross-correlation of a code with the first type of truncation with a test code of the same length, with no data, for  $P=4$  and  $p=1$ . The test code and the truncated code have different initial fills.

TABLE 8: Parameters of the Peak Formation Process of  
Figures 18 and 19 with  $P=4$  and  $p=1$

Peak Number	beginning of formation on the detector	duration	end of formation
1	$-(p+P)=-5$	$p=4$	$-p=-1$
2	$-(p+P)/2=-2.5$	$p=4$	$(-p+P)/2=1.5$
3	0	$p=4$	$P=4$
4	0	$p=4$	$P=4$
5	$(p+P)/2=2.5$	$p=4$	$(p+3P)/2=6.5$
6	$3(p+P)/2=5$	$p=4$	$(3p+5P)/2=9$
7	$p+P=5$	$p=4$	$p+2P=9$
8	$3(p+P)/2=7.5$	$p=4$	$(3p+5P)/2=11.5$
9	$2(p+P)=10$	$p=4$	$2p+3P=14$

The amount of time when there is growth depends on the length of the truncation and on where the initial fill of the test code occurs relative to the beginning of the truncated code. The integration time has to be adjusted accordingly. An extreme case would be the cross-correlation of a modified code with 50% truncation with a test code whose initial fill is such that the wrong half of the code is used to perform the cross-correlation. No correlation peak would result.

#### 4.4 Determination of the Characteristics of the Truncation

The previous analysis provides tools to extract information about the truncation from the characteristics of the peak patterns generated by the autocorrelation of the truncated code and by the cross-correlation between the truncated code and the original code or a test code.

##### 4.4.1 Length of the Truncated Segment

Three different methods are possible to evaluate the length of a truncated code. Using the first method, the autocorrelation allows the evaluation of the period of the peak train and consequently, the length of the truncation if there is no data. The integration time  $T_i$  should be set to a value that produces enough gain to allow the detection of two successive peaks. When data is present, the build-up of multiple peaks is possible if the integration time necessary to produce trains of

detectable peaks is shorter than half the data duration; in this case the integration interval does not usually contain a data transition. However, when longer integration times are required, the presence of data destroys the peak pattern and no information can be obtained with that technique.

It is also possible to evaluate the amount of truncation from the shift between the different trains of peaks in the cross-correlation of the truncated signal with the original code. The peak formation process is not synchronized with the detector integration period, so it is necessary to increase the integration time to allow the formation of the peaks of interest with maximum height. In that case, the integration time should be at least four times the code duration to allow the formation of two peaks from two successive trains.

If it is desired to have access to larger integration times and better gains, it is necessary to remove the shift between the various peak trains. It can be done by performing the cross-correlation with a test code having the same length as the truncated code. If the number of chips truncated from the test code is the same as for the truncated code, the drifting of the peak pattern associated with the successive trains of peaks disappears. However, a difficulty may appear because energy does not accumulate all the time. The periods of growth are followed by periods where no energy accumulates in the peak. The amount of time when there is growth depends on the length of the truncation and on where the initial fill of the test code occurs relative to the beginning of the truncated code. The integration time has to be adjusted accordingly. An extreme case would be the cross-correlation of a modified code with 50% truncation with a test code whose initial fill is such that the wrong half is used to perform the cross-correlation. No correlation would result.

#### 4.4.2 Initial Fill Determination.

If the S/N is very good, it is possible to find the initial fill of the truncated code and subsequently, which chips have been removed, by the following procedure.

It is assumed that the length of the truncation is known and that the truncation is at the end of the code. The procedure consists of trying, one after the other, all possible initial fills, thus generating all the corresponding test codes. For each test code, a cross-correlation is performed with the truncated code. The same segment of the truncated code has to be used for all trials and the integration time should be  $p$ , the duration of the truncated code. The tallest correlation peak is associated with the correct initial fill because in that case all the chips of the test code contribute to the peak. If the initial fill is wrong, the test code will not start at the right



location, a few chips of the test code will not be identical to the given truncated code and a smaller peak will be observed. This is generally useful only if the S/N is very good.

## 5.0 SECOND TYPE OF CODE TRUNCATION

The second type of code truncation consists of signals that contain a full period of the original code AB followed by a partial repetition AX of the original code (see Figure 11b and Figure 20). For the purpose of analysis, the period of the original signal AB is defined as  $P$ , the code AB is divided into two segments AX and XB of durations  $D$  and  $d$  respectively and the truncated code has a period of  $P+D$ .

The patterns produced by the autocorrelation and the cross-correlation with the original code or a test code are more complex than those of the augmented or the truncated cases studied in the previous sections. The reason for the increased complexity is that the segment AX appears twice in the truncated code and generates supplementary correlation peaks both in the autocorrelation and in the cross-correlation with the original code or with a test code.

### 5.1 Autocorrelation

Three types of peak trains (see Figure 20) can be observed in the autocorrelation of the truncated code. One of the peak trains contains tall peaks, the two other peak trains are made up of smaller peaks. They have the same period, but are shifted relative to one another.

The peaks of row III, IV and V illustrate the first type of peak train. They are similar in origin and properties as the other autocorrelation peaks studied earlier in this document. The period of the trains,  $(P+D)/2$ , is determined by the length of the truncated code divided by two. The build-up time of the peaks is  $P+D$ , the duration of the truncated code.

Let us examine, for rows III, IV and V, the chronology of events (see Figure 21 and Table 9) within the time-delay window of width  $P+D$  indicated by vertical lines on Figures 20 and 21. Peak #1 starts formation at  $t=-(P+D)=-10$  and terminates formation at  $t=0$  so it does not contribute to the energy accumulated by the detector for the integration period starting at  $t=0$ . It has been illustrated only for the sake of completeness because it is at the same location as peak #4 and #7. The formation of peak #4 starts at  $t=0$  when the formation of peak #1 ends, and finishes at  $t=P+D=10$ . The formation of peak #7 that is located at the same location than peak #1 and #4, begins at  $t=P+D=10$ , when the formation of peak #4 ends. So there is a continuous accumulation of energy at the corresponding location in the time-delay window.

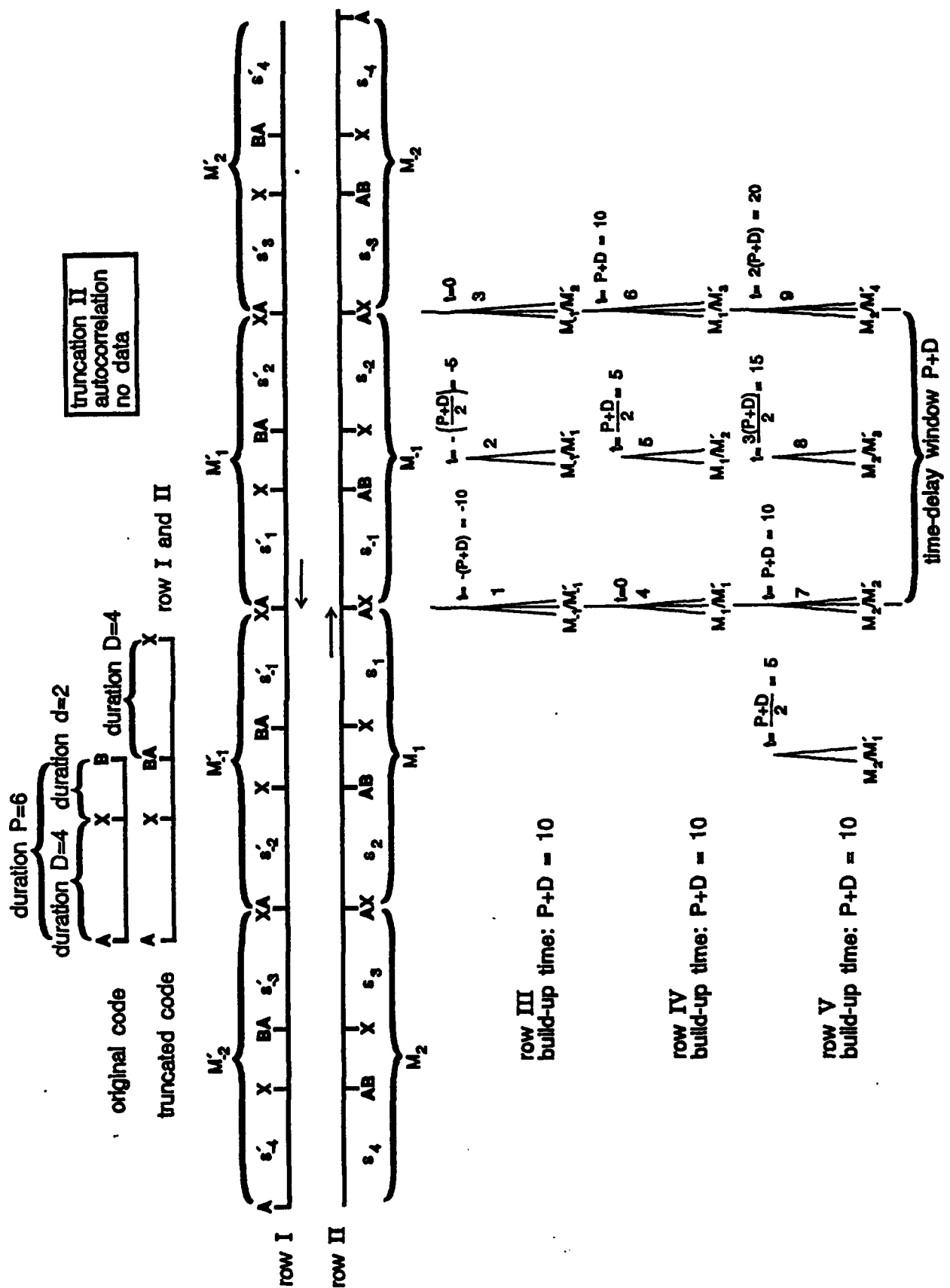
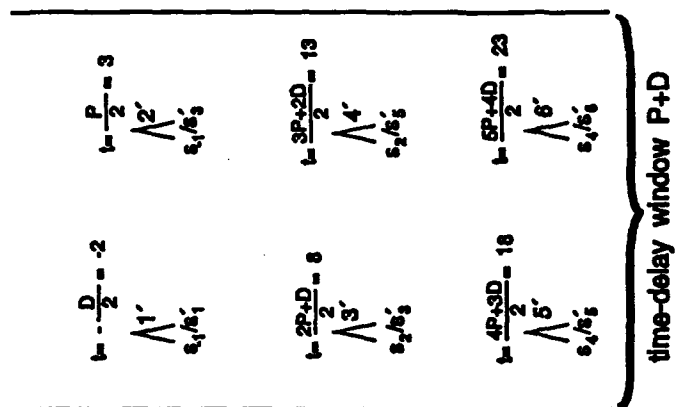


Figure 20: Autocorrelation of a code with a truncation of the second type, with no data, for  $P=6$ ,  $D=4$  and  $d=2$ .

row VI  
build-up time: D = 4

row VII  
build-up time: D = 4

row VIII  
build-up time: D = 4



$$t = \frac{P}{2} = 3$$

$$\bigwedge_{s_2/s_1'}$$

$$t = \frac{2P+D}{2} = 8$$

$$\bigwedge_{s_3/s_1'}$$

$$t = \frac{3P+2D}{2} = 13$$

$$\bigwedge_{s_4/s_2'}$$

Figure 20:  
(cont'd)

Autocorrelation of a code with a truncation of the second type, with no data, for P=6, D=4 and d=2.

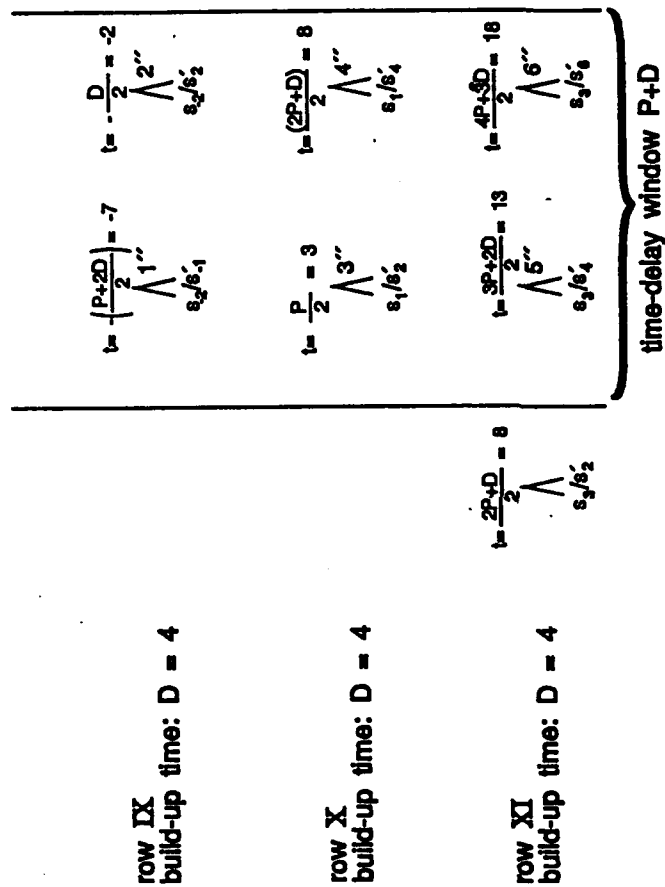


Figure 20:  
(cont'd)

Autocorrelation of a code with a truncation of the second type, with no data, for P=6, D=4 and d=2.

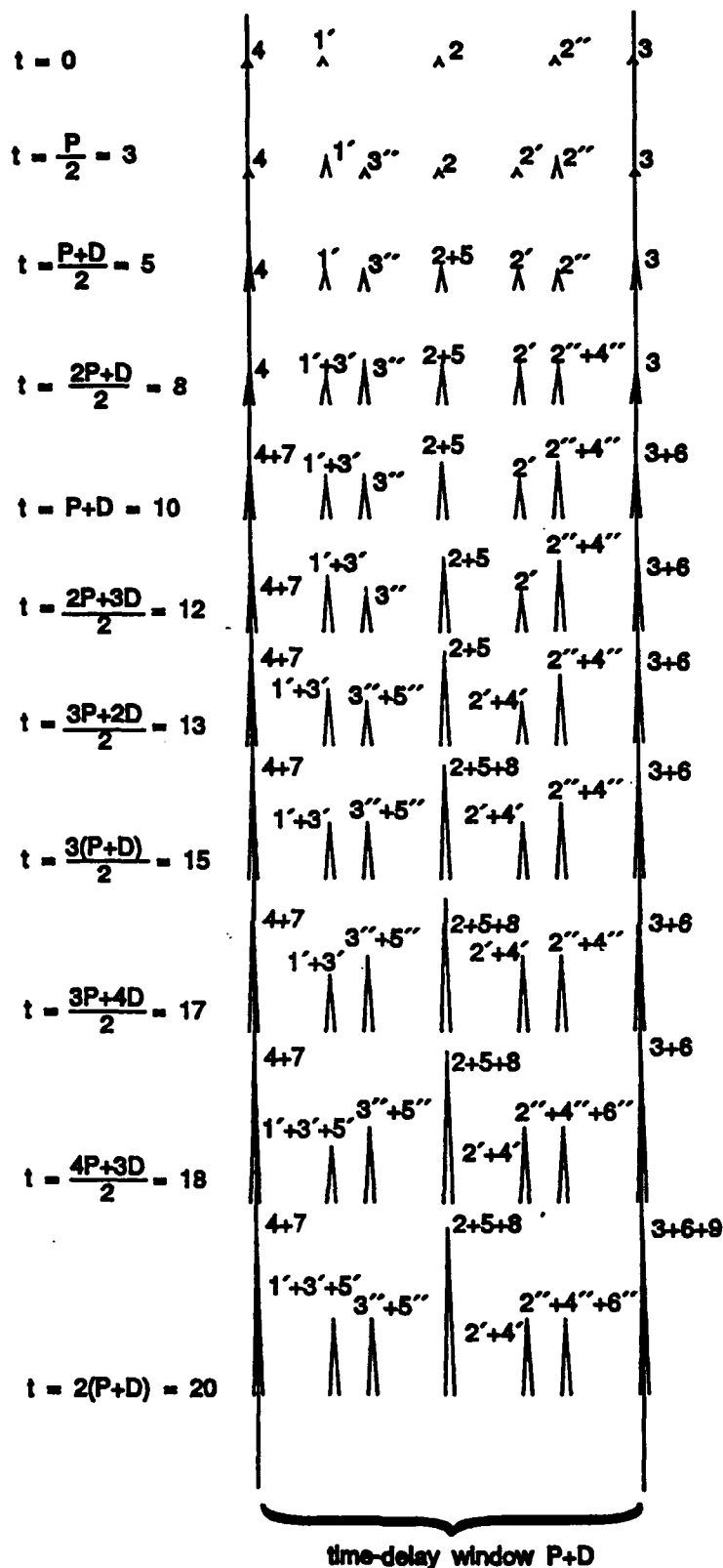


Figure 21: Chronology of peak formation for the autocorrelation of a code with a truncation of the second type with the original code, with no data, for  $P=6$ ,  $D=4$  and  $d=2$ .

A similar phenomenon can be observed at two other locations, for peaks #2, #5 and #8 and for peaks #3, #6 and #9 where there is accumulation of energy without interruption during the integration period.

The second and third types of peaks are illustrated respectively in rows VI, VII, VIII and in rows IX, X and XI of Figure 20. In order to avoid confusion, the number for the second type of peak train in rows VI, VII and VIII have a "'" and the third type of peak train in rows IX, X and XI have a """. They are supplementary short peaks generated by the autocorrelation of segments AX and they are unique to the second type of truncation. Their build-up time is the duration  $D=4$  of the AX segment so their height is smaller than the ordinary autocorrelation peak whose height is proportional to  $P+D=10$ ; however, the period of these peak trains is  $(P+D)/2=5.5$ , the same as for the tall train of peaks. These peaks accumulate energy during only a fraction of the integration time.

Let us look at the sequence of events taking place in the time-delay window indicated on Figures 20 and 21 for the second type of peaks. Peak #1' begins and terminates its formation at  $t=-D/2=-2$  and  $t=D/2=2$ , respectively. It contributes energy to the integration interval from  $t=0$  to  $t=D/2=2$ . Peak #3' is at the same location as peak #1' and begins formation at  $t=(2P+D)/2=8$  and ends at  $t=(2P+3D)/2=12$ . Peak #5' is also at the same location as peaks #1' and #3' and starts formation at  $t=(4P+3D)/2=18$  and ends at  $t=(4P+5D)/2=22$ . Periods of growth of duration  $D$  alternate with periods of height stability of duration  $P$ . A similar process takes place for the formation of the third type of peak trains of rows IX, X and XI. The second and third trains of peaks are shifted respectively by a distance  $D/2$  and  $P/2$  from the train of tall peaks thus giving an indication of the structure of the truncated code. However, it is not possible to monitor this process. The only access to the data comes from the read-out of the detector array that gives the results of the energy integration that has taken place during the integration time  $T$  prior to the read-out.

The presence of the short and tall trains of peak has to be established in order to produce the warning of the presence of the second type of truncation and the integration time has to be adjusted to produce a gain that is sufficient to allow the detection of the three types of peaks given the S/N of the input signal. Failure to detect the presence of the trains of short peaks could lead to erroneous evaluations of the length of the original code and of the type of truncation.

TABLE 9: Parameters of the Peak Formation Process of  
Figures 20 and 21 with  $P=6$ ,  $D=4$  and  $d=2$

Peak Number	beginning of formation on the detector	duration	end of formation
1	$-(P+D)=-10$	$P+D=10$	0
2	$-(P+D)/2=-5$	$P+D=10$	$(P+D)/2=5$
3	0	$P+D=10$	$P+D=10$
4	0	$P+D=10$	$P+D=10$
5	$(P+D)/2=5$	$P+D=10$	$3(P+D)/2=15$
6	$P+D=10$	$P+D=10$	$2(P+D)=20$
7	$P+D=10$	$P+D=10$	$2(P+D)=20$
8	$3(P+D)/2=15$	$P+D=10$	$5(P+D)/2=25$
9	$2(P+D)=20$	$P+D=10$	$3(P+D)=30$
1'	$-D/2=-2$	$D=4$	$D/2=2$
2'	$P/2=3$	$D=4$	$(2D+P)/2=7$
3'	$(2P+D)/2=8$	$D=4$	$(2P+3D)/2=12$
4'	$(3P+2D)/2=13$	$D=4$	$(3P+4D)/2=17$
5'	$(4P+3D)/2=18$	$D=4$	$(4P+5D)/2=22$
6'	$(5P+4D)/2=23$	$D=4$	$(5P+6D)/2=27$
1''	$-(P+2D)/2=-7$	$D=4$	$(P+4D)/2=-3$
2''	$-D/2=-2$	$D=4$	$D/2=2$
3''	$P/2=3$	$D=4$	$(P+2D)/2=7$
4''	$(2P+D)/2=8$	$D=4$	$(2P+3D)/2=12$
5''	$(3P+2D)/2=13$	$D=4$	$(3P+4D)/2=17$
6''	$(4P+3D)/2=18$	$D=4$	$(4P+5D)/2=22$

## 5.2 Cross-Correlation with the Original Code

The peak patterns generated by the cross-correlation of the truncated code with the original code are quite complex. The problem is that there is no longer any alignment of the different peak trains as was the case for the autocorrelation. All of the peak trains are shifted relative to each another. However, information is contained in the shifts of the different peak trains and it can be used to characterize the truncated code if the S/N of the truncated code is sufficient.

### 5.2.1 With the Same Initial Fill

When a truncated code and an original code having the same initial fill are cross-correlated, two types of peak trains with the same amplitude are formed. However, the successive peak trains of the same type do not overlap and their interleaving produces complex peak patterns.

The formation of the first type of peak trains is illustrated in row III, row IV and row V of Figure 22. Although successive trains have the same period  $P$  and the same build-up time  $P+D$ , they are shifted by a quantity  $d/2$  that corresponds to the amount missing from the second repetition of the original code in the truncated code (see Table 10).

The second type of peak train is illustrated in rows VI, VII and VIII of Figure 22. The peak numbers have a "1" to avoid confusion with the first type of train. They belong to different peak trains that do not overlap. The period of the peak trains is  $(P+p)/2$  and their peak build-up time is  $P+D$ . The shift between the train of peaks is also  $d/2$  as for the tall peaks of rows III, IV and V.

The integration time  $T_i$  required to reveal the structure of the truncated code should allow the build-up of two full-height peaks from two consecutive peak trains for each type of peak train, so  $T_i > 2.5(P+D)$ .

In order to ensure that the integration time  $T_i$  is large enough to allow the peaks to reach maximum amplitude, another factor  $P+D$  must be added to take into account the unknown synchronization between the integration period and the peak build-up process. So  $T_i > (7P+5D+d)/2$  should be used. However, the build-up time of the short peaks is only  $P+D=7$  and it will be possible to detect the presence of these peaks only if this integration time produces enough gain to allow the detection of the peaks considering the S/N of the truncated code.



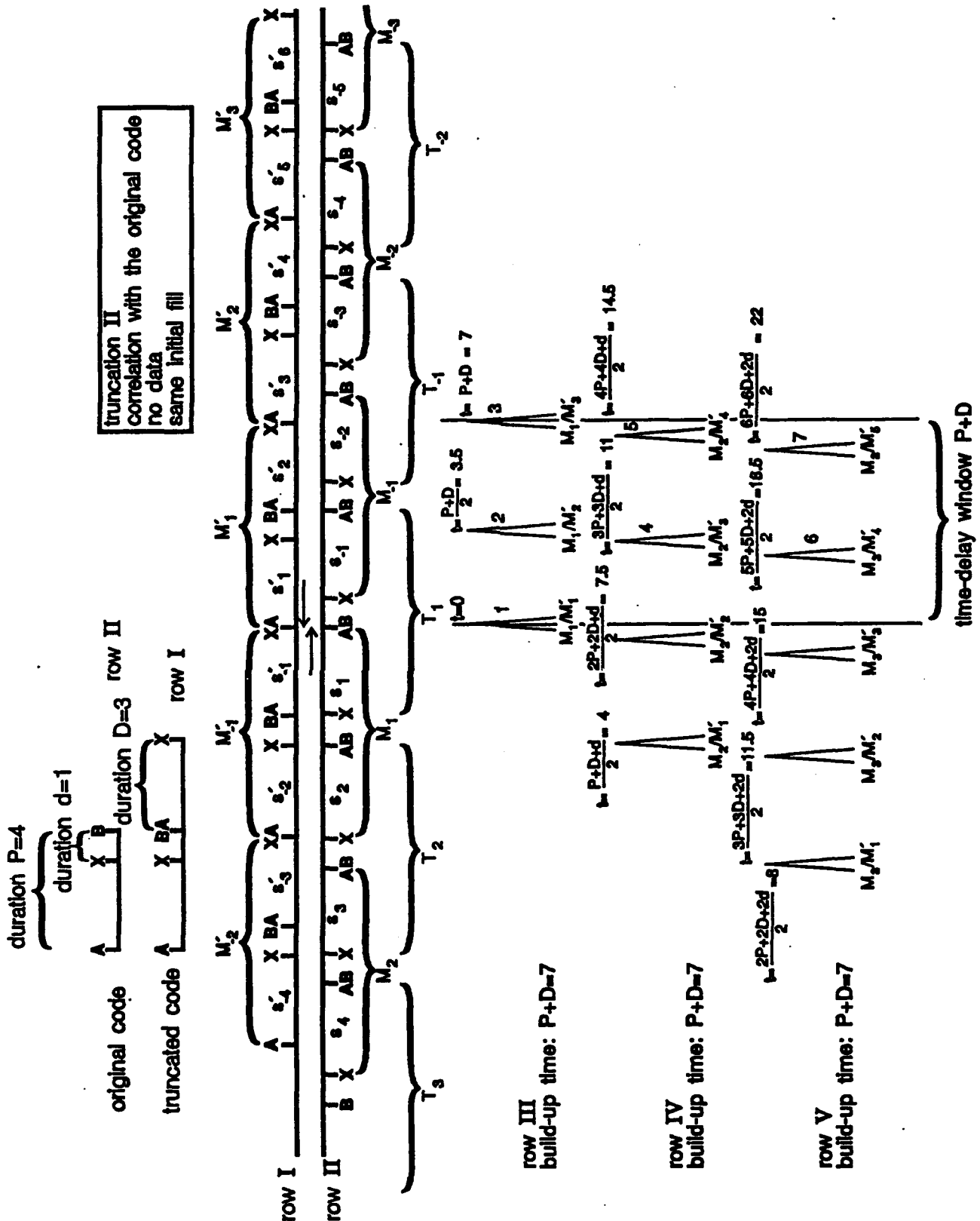


Figure 22:

Cross-correlation of a code with a truncation of the second type with the original code, with no data, for  $P=4$ ,  $D=3$  and  $d=1$ . Both the truncated code and the original code have the same initial fill.

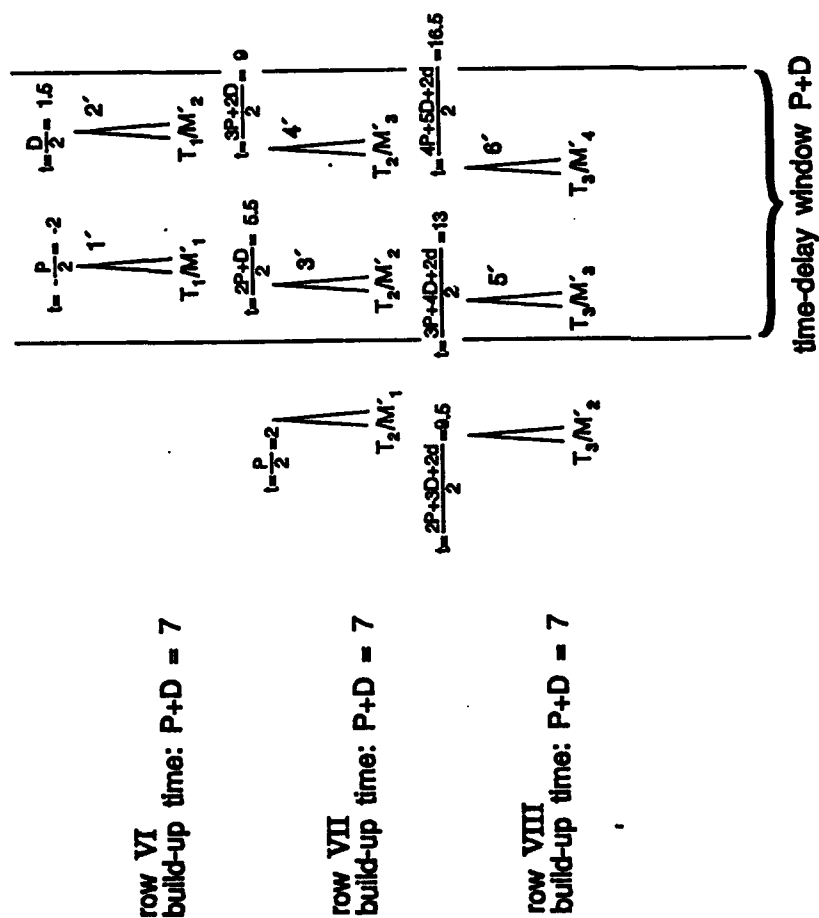


Figure 22:  
(cont'd)

Cross-correlation of a code with a truncation of the second type with the original code, with no data, for  $P=4$ ,  $D=3$  and  $d=1$ . Both the truncated code and the original code have the same initial fill.

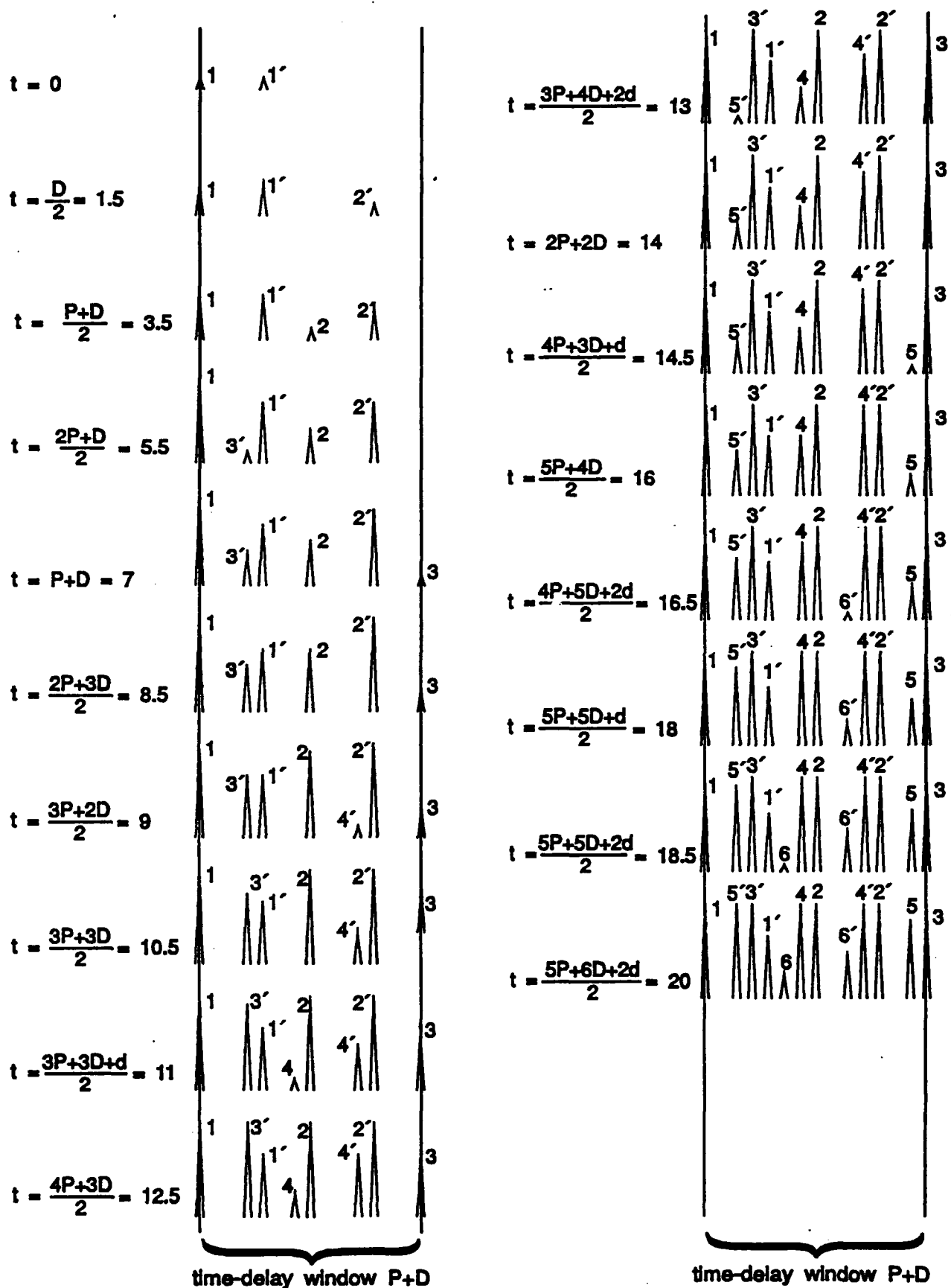


Figure 23:

Chronology of peak formation for the cross-correlation of a code with a truncation of the second type with the original code, with no data, for  $P=4$ ,  $D=3$  and  $d=1$ . The truncated code and the original code have the same initial fill.

TABLE 10: Parameters of the Peak Formation Process of Figures 22 and 23 with  $P=4$ ,  $D=3$  and  $d=1$

Peak Number	beginning of formation on the detector	duration	end of formation
1	0	$P+D=7$	$P+D=7$
2	$(P+D)/2=3.5$	$P+D=7$	$3(P+D)/2=10.5$
3	$P+D=7$	$P+D=7$	$2(P+D)=14$
4	$(3P+3D+d)/2=11$	$P+D=7$	$(5P+5D+d)/2=18$
5	$(4P+4D+d)/2=14.5$	$P+D=7$	$(6P+6D+d)/2=21.5$
6	$(5P+5D+2d)/2=18.5$	$P+D=7$	$(7P+7D+2d)/2=25.5$
7	$(6P+6D+2d)/2=22$	$P+D=7$	$(8P+8D+2d)/2=29$
1'	$-P/2=-2$	$P+D=7$	$(P+2D)/2=5$
2'	$D/2=1.5$	$P+D=7$	$(2P+3D)/2=8.5$
3'	$(2P+D)/2=5.5$	$P+D=7$	$(4P+3D)/2=12.5$
4'	$(3P+2D)/2=9$	$P+D=7$	$(5P+4D)/2=16$
5'	$(3P+4D+2d)/2=13$	$P+D=7$	$(5P+6D+2d)/2=20$
6'	$(4P+5D+2d)/2=16.5$	$P+D=7$	$(6P+7D+2d)/2=23.5$

### 5.2.2 With Different Initial Fills

The truncated and the original code are illustrated in the top-left part of Figure 24. The original code starts at A and ends at B. The starting point of the truncated code is designated by the letter V and the letter Y designates the end of the truncated code. The location of points V and Y is also indicated on the original code.

The cross-correlation of a truncated code of the second type with the original code, when they have different initial fills (see Figures 24 and 25 and Table 11) produces trains of tall and short peaks that are shifted relative to one another. Information is contained in the presence of the trains of short peaks and in the shifts of the different peak trains and it can be used to characterize the truncated signal if the S/N is good enough. Three types of peak trains are produced.

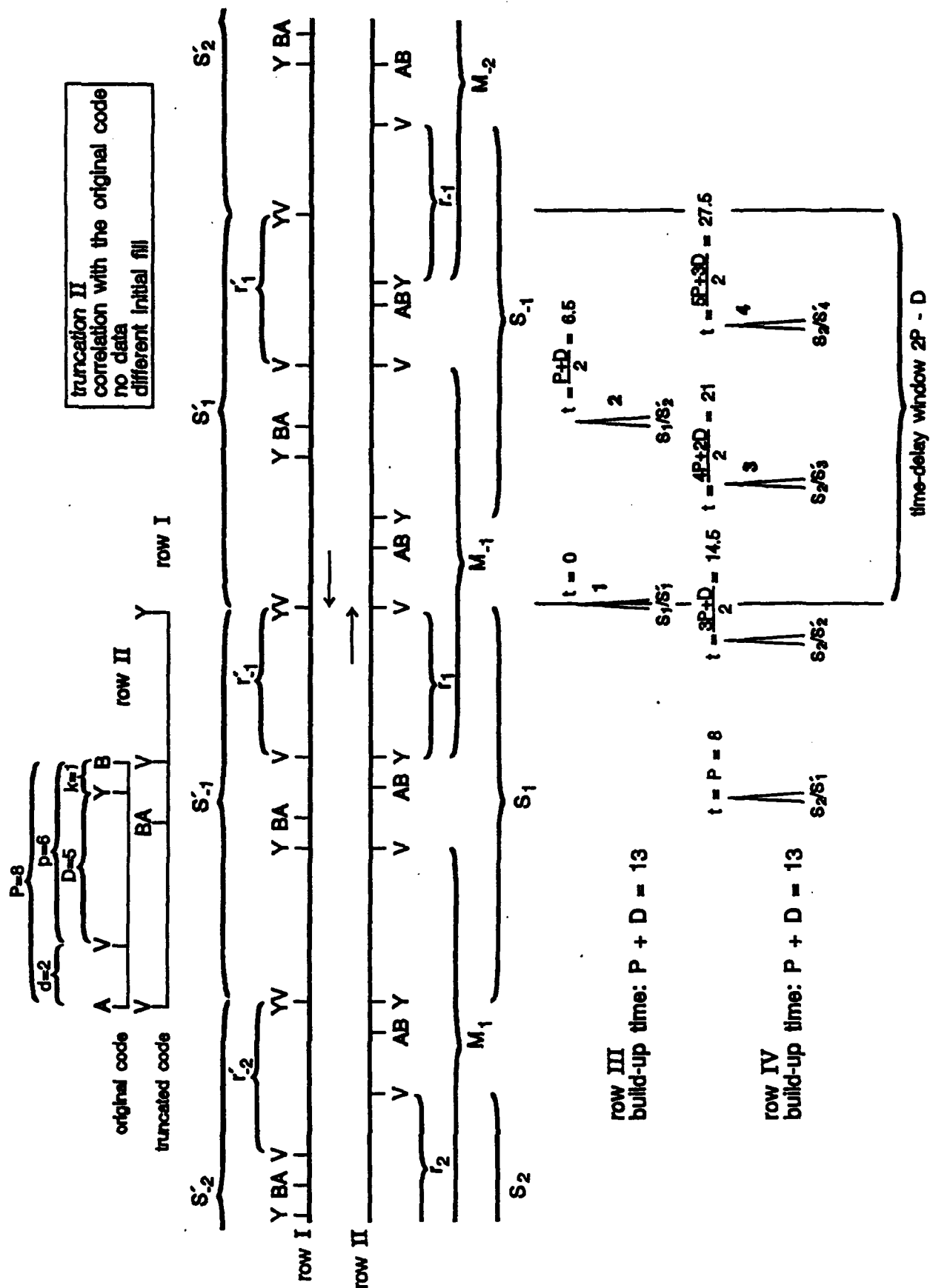
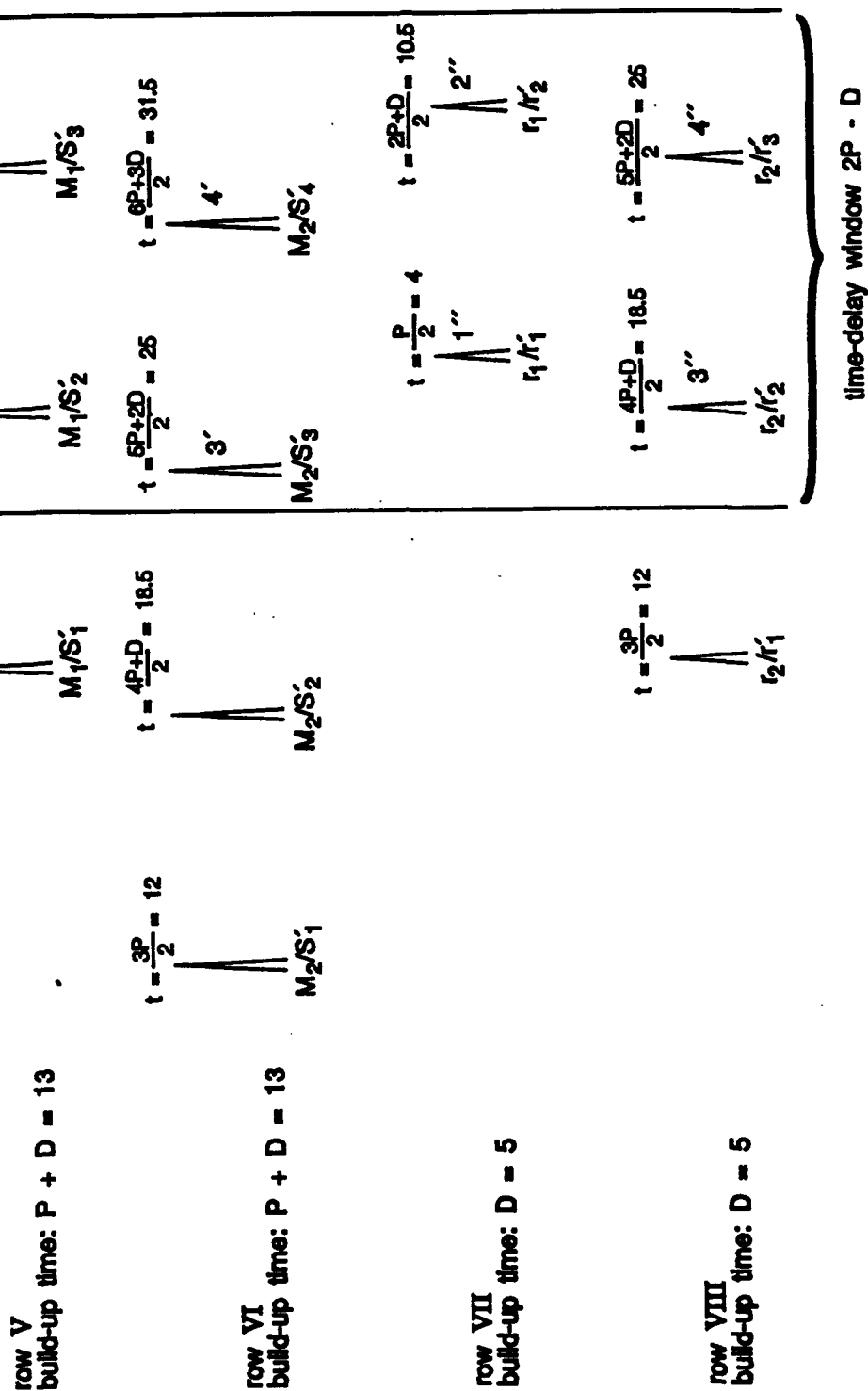


Figure 24:

Cross-correlation of a code with a truncation of the second type with the original code, with no data, for  $P=8$ ,  $D=5$ ,  $p=6$ ,  $d=2$  and  $k=1$ . Both the truncated code and the original code have different initial fills.

Figure 24:  
(cont'd)



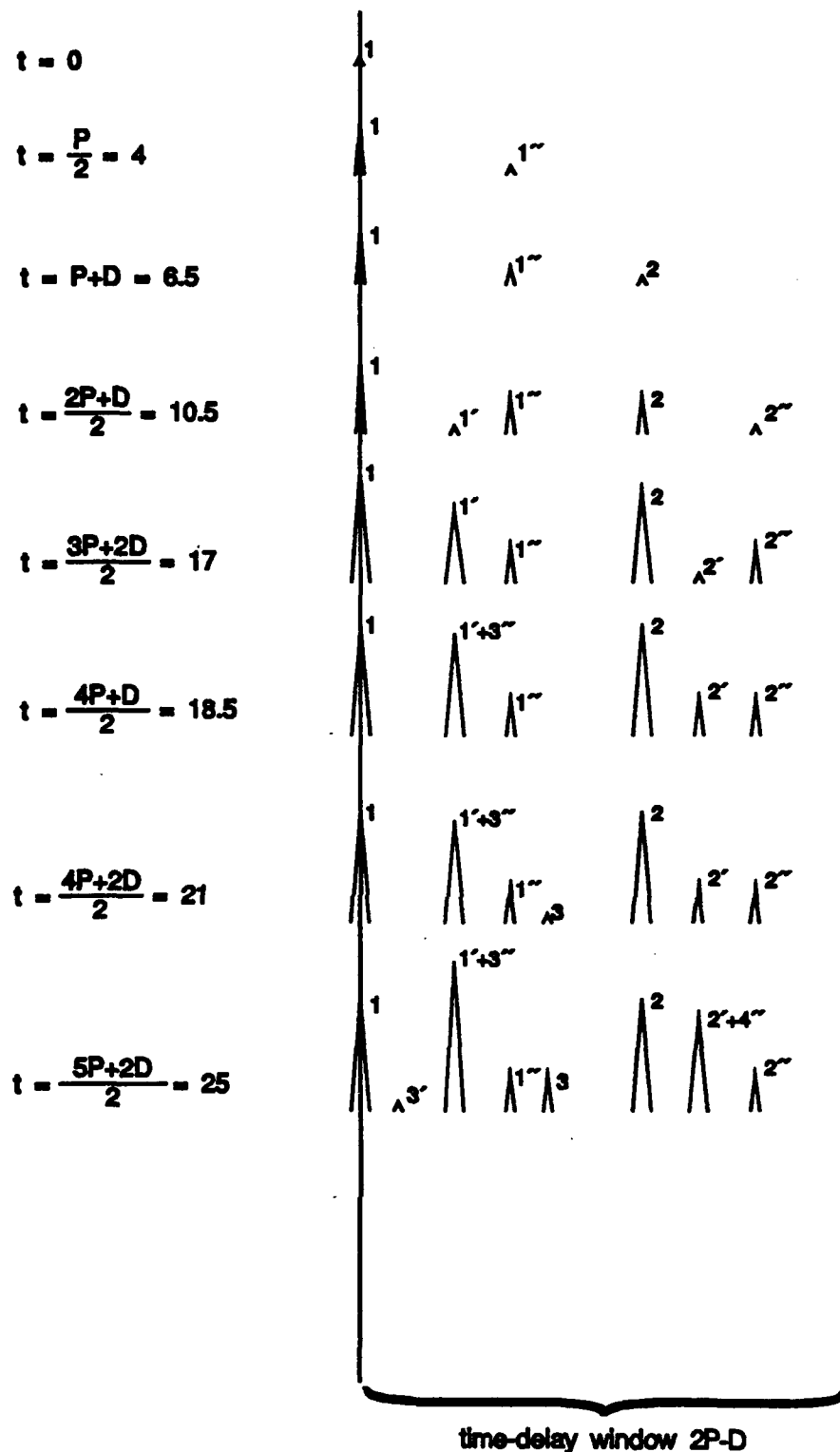


Figure 25: Chronology of peak formation for the cross-correlation of a code with a truncation of the second type with the original code, with no data, for  $P=8$ ,  $D=5$ ,  $p=6$ ,  $d=2$  and  $k=1$ . The truncated code and the original code have different initial fills.

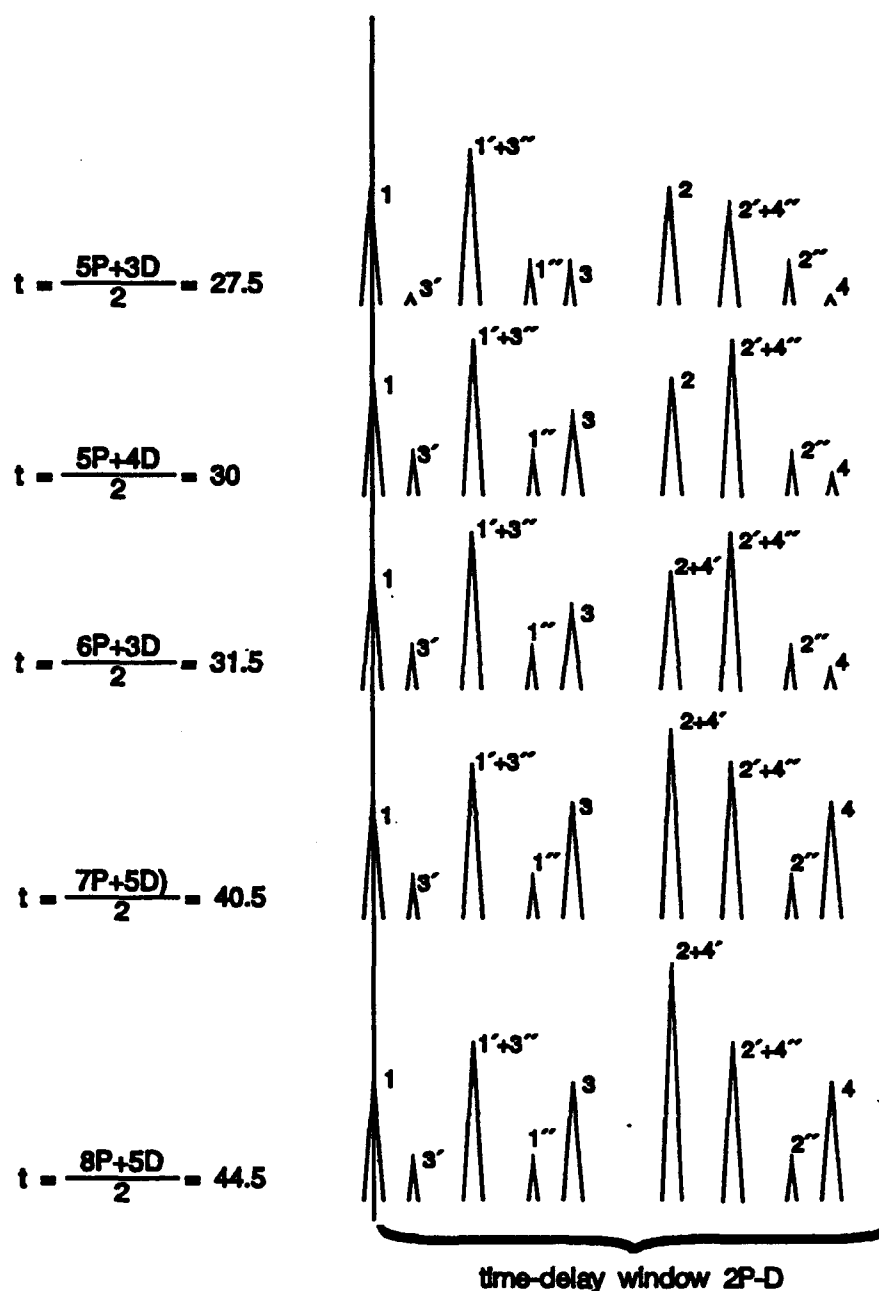


Figure 25:  
(cont'd)

Chronology of peak formation for the cross-correlation of a code with a truncation of the second type with the original code, with no data, for  $P=8$ ,  $D=5$ ,  $p=6$ ,  $d=2$  and  $k=1$ . The truncated code and the original code have different initial fills.



TABLE 11: Parameters of the Peak Formation Process of  
Figures 24 and 25 with  $P=8$ ,  $D=5$ ,  $p=6$ ,  $d=2$  and  $k=1$

Peak Number	beginning of formation on the detector	duration	end of formation
1	0	$P+D=13$	$(P+D)/2=13$
2	$(P+D)/2=6.5$	$P+D=13$	$3(P+D)/2=18.5$
3	$(4P+2D)/2=21$	$P+D=13$	$(6P+4D)/2=34$
4	$(5P+3D)/2=27.5$	$P+D=13$	$(7P+5D)/2=40.5$
1'	$(2P+D)/2=10.5$	$P+D=13$	$(4P+3D)/2=23.5$
2'	$(3P+2D)/2=17$	$P+D=13$	$(5P+4D)/2=30$
3'	$(5P+2D)/2=25$	$P+D=13$	$(7P+4D)/2=38$
4'	$(6P+3D)/2=31.5$	$D=5$	$(8P+5D)/2=44.5$
1''	$P/2=4$	$D=5$	$(P+2D)/2=9$
2''	$(2P+D)/2=10.5$	$D=5$	$(2P+3D)/2=15.5$
3''	$(4P+D)/2=18.5$	$D=5$	$(4P+3D)/2=23.5$
4''	$(5P+2D)/2=25$	$D=5$	$(5P+4D)/2=30$

The formation of the first type of peak train is illustrated in rows III and IV of Figure 24. Although the trains have the same period  $(P+D)/2$  and the same build-up time  $P+D$ , they are shifted by a quantity  $(k+d)/2$  that corresponds to the amount missing from the second repetition of the original code (see Table 11).

The second type of peak train is illustrated in rows V and VI of Figure 24. The peak numbers have a "'" to avoid confusion with the first type of peak train. They belong to different peak trains that do not overlap. The period of the peak trains is  $(P+D)/2$  and their build-up time is  $P+D$ . The shift between the train of peaks is also  $(k+d)/2$  as for the tall peaks of rows III and IV. Peak #1' is first formed (see Figure 24) but peak #3' is not located in the same position as peak #1'; it belongs to another shifted train of peaks. Similarly, peak #4' is also shifted by  $(k+d)/2$  from the location of peak #2'.

The third type of peak train is illustrated in rows VII and VIII of Figure 24. These peaks have a build-up time of  $D$  and are consequently lower than the peaks of the first and second type of train just discussed. These types of peak train are

characterized by alternating intervals of peak growth and constant height. The period of the peak trains is  $P$  and the shift between the trains of peaks is also  $(k+d)/2$  as for the tall peaks of rows III, IV, V and VI.

Peak #1" is the first one being formed. After an interval when no energy is contributed to any of the peaks of the third type of train, the peak #2" is formed followed by a period when no energy accumulates in any of the peaks.

The integration time  $T_i$  required to reveal the structure of the truncated code should allow the build-up of two consecutive peak trains containing two consecutive peaks for the three types of peak trains; hence, it is required that  $T_i > (5P+4D)/2$ . In order for the integration time  $T_i$  to be large enough to allow the peaks to reach maximum amplitude, another factor  $P+D$  has to be added to take into account the unknown synchronization between the integration period and the peak build-up process; so  $T_i$  should be greater than  $(7P+6D)/2$ .

However, the build-up time of the short peaks is only  $D=7$  and it will be possible to detect the presence of these peaks only if this integration time produces enough gain to allow the detection of the peaks considering the S/N of the truncated code.

### 5.3 Cross-Correlation with a Test Code

Let us define the test code associated with a truncated code of the second type as the code formed by the concatenation of the original code with a truncated repetition of itself. The repetition is truncated in such a way as to produce a test code of the same length as the truncated code of the second type.

#### 5.3.1 With the Same Initial Fill

The cross-correlation of the truncated code with a test code of the same length that has the same initial fill produces the same peak patterns as the autocorrelation described in Section 5.1. However, the peaks are easier to detect because the test code does not contain any noise and the integration time required to produce enough gain to overcome the noise should be reduced by a factor of two from what is required for the autocorrelation case.

#### 5.3.2 With Different Initial Fills

A truncated code and a test code with different initial fills are illustrated in Figure 26. The original code starts at point A and ends at point B. The truncated code contains a full period AB of the original code concatenated to a partial repetition AX of the original code. The test code has the same length as the truncated code but starts at point V and ends at

point Y. All the starting or ending points of either the truncated or the test code are indicated on the three codes illustrated.

When the truncated code and the test code have different initial fills, shifted trains of peaks of different height are formed and the growth patterns become more complicated. Three types of trains containing peaks of different height are observed.

Rows III and IV illustrate the formation of the first train of peaks. Peak #1 starts formation at  $t=d/2=1$  and continues to accumulate energy until  $t=(2P+2p+d)=12$ . An interval of length  $d=2$  without peak growth follows and later peak #3 adds another contribution to the peak.

The formation of the second peak train is illustrated in rows V and VI. These peaks are designated by numbers accompanied by "'". This peak train contains medium height peaks originating from the interaction of short segments of the codes being cross-correlated. The contribution illustrated in row VI for peak #1' has a duration of  $t=P-k=7$  and is followed by a second contribution from peak #3' after an interval during which no energy is contributed to the peak. The total energy contributed to the peak is proportional to  $P-k$ . The process just described repeats for peaks #2' and 4'. This peak train is shifted by  $(p+d)/2$  from the train of tall peaks.

The third type of peak train is illustrated in rows VII and VIII of Figure 26 and the peaks are designated by numbers with a " ". It is a train of short peaks whose formation time is proportional to the duration of the segment of length  $p$ . This peak train is shifted by a distance  $P/2$  from the train of tall peaks.

The integration time  $T_i$  required to reveal the structure of the truncated code should allow the build-up of two full-height peaks from two consecutive trains for each type of peak train, from the beginning of the formation of peak #1 to the end of formation of peak #4",  $T_i > (5P+5d+6p-d)/2$ .

In order to ensure that the integration time  $T_i$  is large enough to allow the peaks to reach maximum amplitude, another factor  $P+D$  has to be added to take into account the unknown synchronization between the integration period and the peak build-up process. So  $T_i > (7P+7d+6p-d)/2$  should be used. However, the build-up time of the short peaks is only  $p=3$  and it will be possible to detect the presence of these peaks only if this integration time produces enough gain to allow the detection of the peak considering the  $S/N$  of the truncated code.

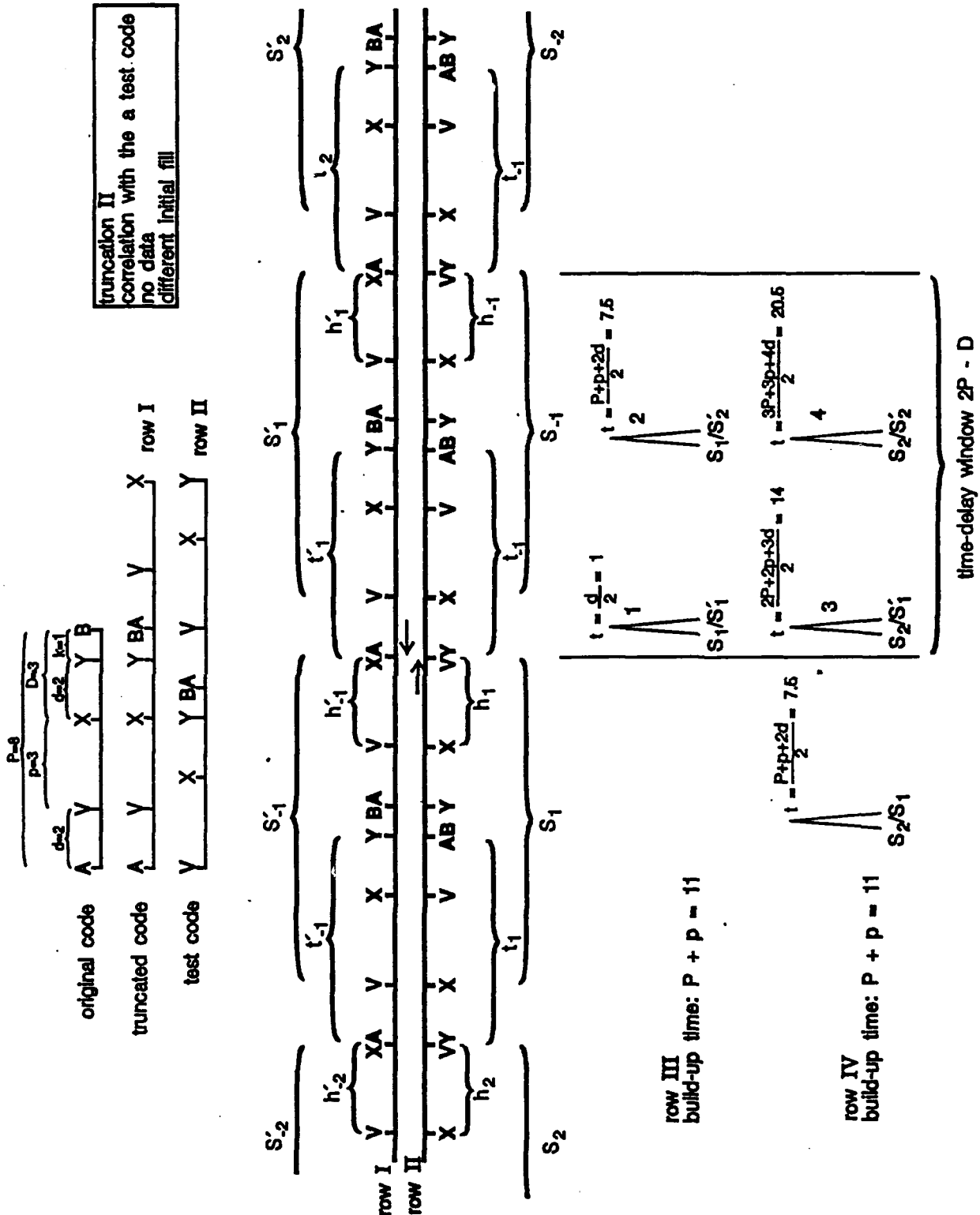


Figure 26:

Cross-correlation of a code with a truncation of the second type with a test code, with no data, for  $P=8$ ,  $D=3$ ,  $p=3$ ,  $d=2$  and  $k=1$ . Both the truncated code and the original code have different initial fills.

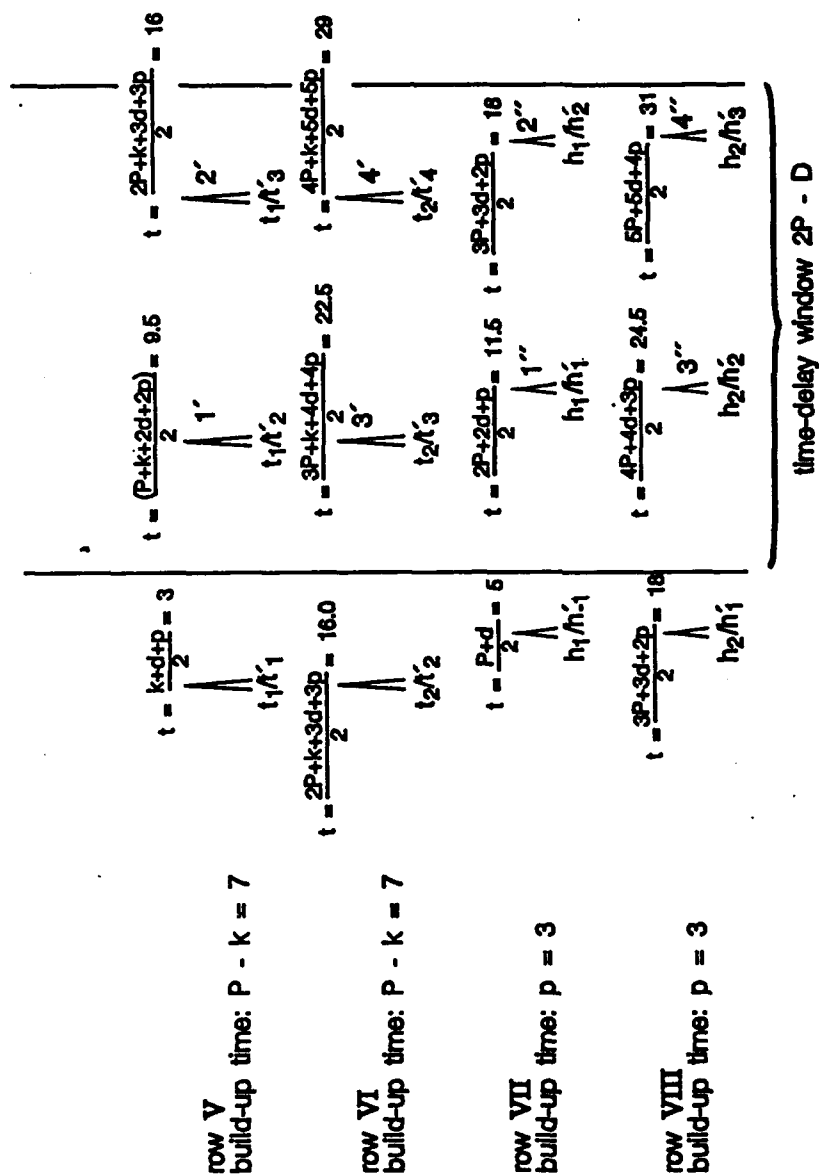


Figure 26:  
(cont'd)

Cross-correlation of a code with a truncation of the second type with a test code, with no data, for  $P=8$ ,  $D=3$ ,  $p=3$ ,  $d=2$  and  $k=1$ . Both the truncated code and the original code have different initial fills.

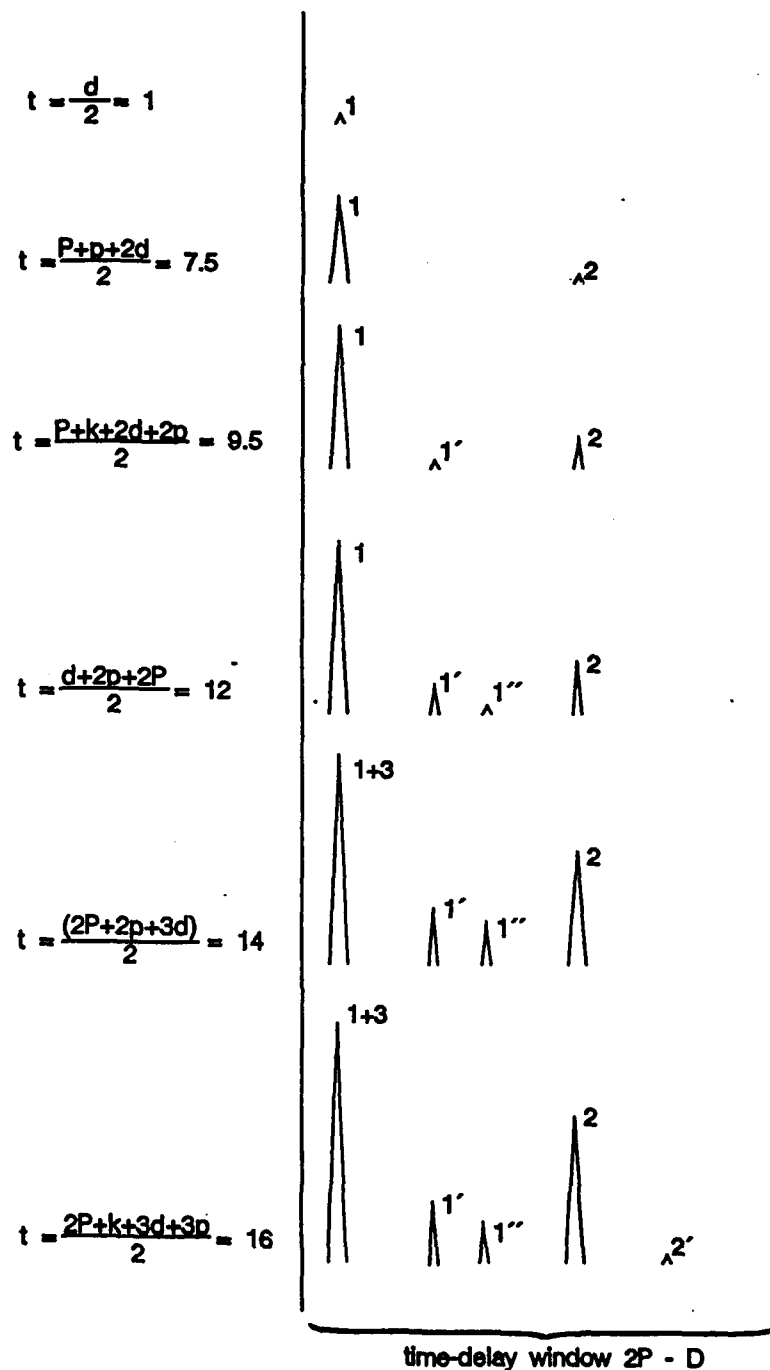


Figure 27:

Chronology of peak formation for the cross-correlation of a code with a truncation of the second type with the original code, with no data, for  $P=8$ ,  $D=3$ ,  $p=3$ ,  $d=2$  and  $k=1$ . The truncated code and the original code have different initial fills.

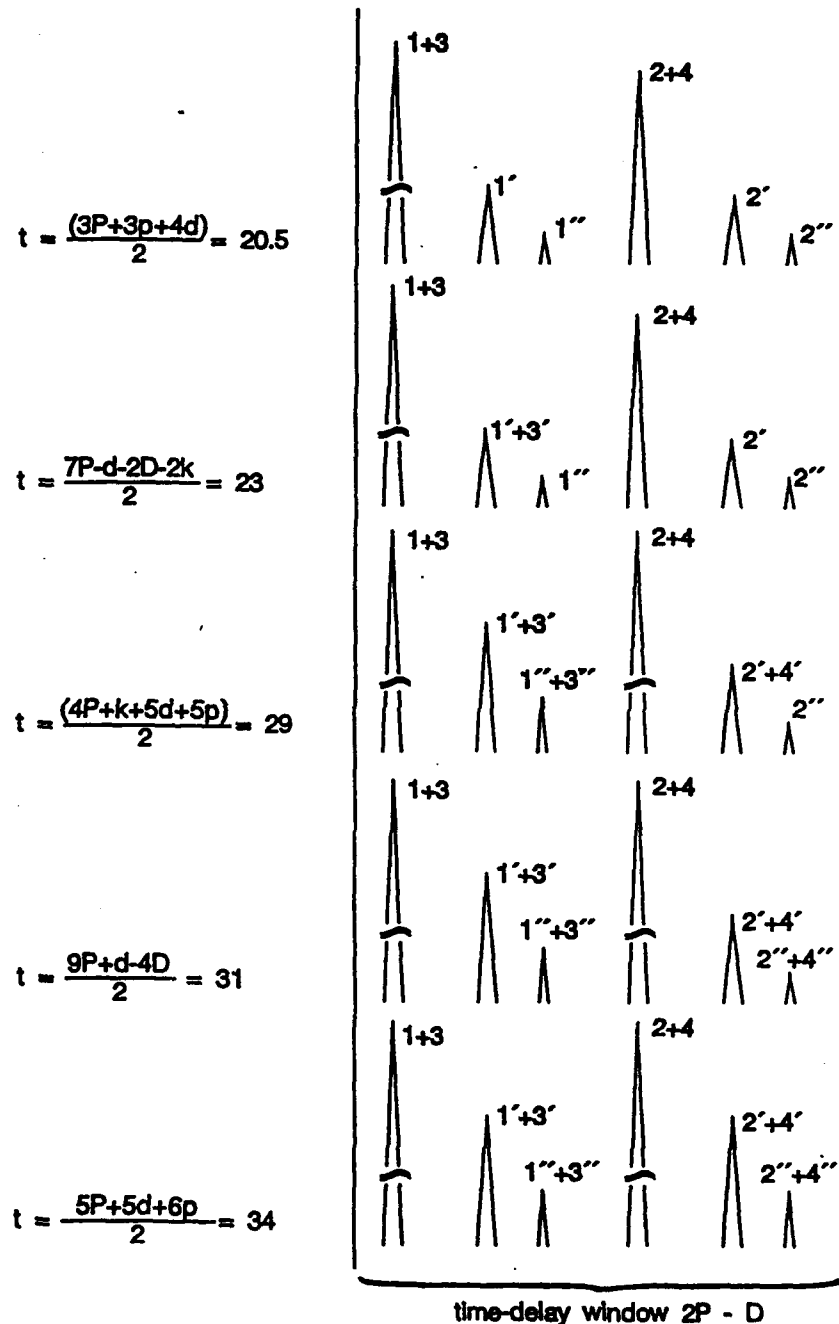


Figure 27:  
(cont'd)

Chronology of peak formation for the cross-correlation of a code with a truncation of the second type with the original code, with no data, for  $P=8$ ,  $D=3$ ,  $p=3$ ,  $d=2$  and  $k=1$ . The truncated code and the original code have different initial fills.

TABLE 12: Parameters of the Peak Formation Process of  
Figures 26 and 27 with  $P=8$ ,  $p=3$ ,  $D=3$ ,  $d=2$  and  $k=1$

Peak Number	beginning of formation on the detector	duration	end of formation
1	$d/2=1$	$P+p=11$	$(d+2p+2p)/2=12$
2	$(P+p+2d)/2=7.5$	$P+p=11$	$(3P+3p+2d)/2=18.5$
3	$(2P+2p+3d)/2=14$	$P+p=11$	$(4P+4p+3d)/2=25$
4	$3P+3p+4d)/2=20.5$	$P+p=11$	$(5P+5p+4d)/2=31.5$
1'	$(P+k+2d+2p)/2=9.5$	$P-k=7$	$(3P-k+2d+2p)/2=16.5$
2'	$(2P+k+3d+3p)/2=16$	$P-k=7$	$(4P-k+3d+3p)/2=23$
3'	$(3P+k+4d+4p)/2=22.5$	$P-k=7$	$(5P-k+4d+4p)/2=29.5$
4'	$(4P+k+5d+5p)/2=29$	$P-k=7$	$(6P-k+5d+5p)/2=36$
1''	$(2P+2d+p)/2=11.5$	$p=3$	$(2P+2d+3p)/2=14.5$
2''	$(3P+3d+2p)/2=18$	$p=3$	$(3P+3d+4p)/2=21$
3''	$(4P+4d+3p)/2=24.5$	$p=3$	$(4P+4d+5d)/2=27.5$
4''	$(5P+5d+4p)/2=31$	$p=3$	$(5P+5d+6p)/2=34$

#### 5.4 Determination of the Characteristics of the Truncation

The peak pattern resulting from the interleaving of shifted trains of peaks has a complex structure that contains information about the amount of truncation and the fact that the second repetition of the initial code has been truncated. The previous analysis provides tools to extract some information about the characteristics of the truncated code.

##### 5.4.1 Length of the Truncated Segment.

Three different methods are possible to evaluate the length of the truncated segment. Using the first method, the length of the truncation and the nature of the truncation are determined from the autocorrelation. The period of the tall and short peaks contains the information about the modified code length. The presence of the short peaks indicates that the second type of truncation was used. A failure to recognize that feature could easily lead to a wrong evaluation of the length of the code. If such a mistake were made, the truncated code of a second type will be mistaken for a truncated code of the first type with approximately twice the total length. It is then



important to adjust the integration time to obtain a gain sufficient to identify the presence of the short and tall peaks. The integration time is determined by the S/N of the signal to be processed.

The second method extracts information from the peak pattern generated by the cross-correlation of the truncated code with the original code. The information about the length of the truncation is contained in the shift between the different trains of peaks. The integration time  $T_i$  should be long enough to allow the formation of two peaks from two successive peak trains. A full period  $P+D$  of the truncated code should be added to the integration time to account for the fact that the synchronization between the peak formation process and the start of the integration period is unknown. A total integration time of  $4(P+D)$  is sufficient. However, the build-up time of the shortest peaks is only  $p=3$  and it will be possible to detect the presence of these peaks only if this integration time produces enough gain to allow the detection of the peak considering the S/N of the truncated code.

Both features, the size of the shift between peak trains and the presence of the short peak trains in the autocorrelation, have to be identified and measured in order to draw correct conclusions about the type of modified code that is processed. It is indeed very easy to mistake a code with the second type of truncation for a code with the first type of truncation with twice the length, if presence of the short peak trains is not recognized.

If it is desired to remove the shift between the various peak trains in order to have access to larger integration times and larger gains, it is necessary to perform the cross-correlation with a test code having a truncation on the second repetition. If the amount of truncation is correct, the drifting of the peak pattern associated with the successive trains of peaks will disappear and peak patterns identical to those formed by the autocorrelation will appear. The integration time that will allow the detection of the peak is half the time required for the autocorrelation because the test code is noiseless.

#### 5.4.2 Initial Fill Determination

If the S/N is very good, it is conceptually possible to determine the initial fill and consequently, which chips have been removed from the second repetition of the code, by applying a procedure that is similar to the method described in Section 4.3.2.

The procedure consists of successively trying all possible initial fills, thus generating all the corresponding test codes. It is assumed at this point that the length of the truncation has been determined and that the truncation is at the end of the second repetition of the code. For each test code, the correlation is performed with the truncated code. The same segment of the truncated code has to be used for all trials and the integration time should be  $P+D$ , the duration of the truncated code. When the correct fill is used, a typical autocorrelation pattern containing a train of tall peaks and a train of short peaks is produced (see Figure 20) and the tallest correlation peaks are associated with the use of the correct fill since the chips of the test code contribute to the peak. If the initial fill is wrong, the test code will not start at the correct location; thus, a few chips of the test code will not be identical to the given code and smaller peaks will be observed. A third train of peaks will appear.

## 6.0 CONCLUSION

The characteristics of the output of a TIC processing truncated or augmented codes were studied. It was demonstrated that complex peak patterns are generated and that they contain information about the modification to the code and that it is possible to retrieve some of that information by applying specific processing methods. The four processing methods that were developed can be summarized as follows:

### 6.1 First Method: Autocorrelation of the Modified Code

#### 6.1.1 No Data

The autocorrelation of the modified code produces periodic peak patterns whose period is proportional to the duration of the modified code. The integration time should be adjusted to allow enough gain to recognize the peak patterns and measure their period.

If the code has a truncation of the second type, interleaved trains of short and tall peaks are produced and the gain should be sufficient to allow the measurement of both type of peaks. A failure to recognize the presence of the train of short peaks would lead to an error in the evaluation of the length of the code and in the nature of the truncation. The integration time has to be sufficient to produce enough gain to allow the detection of the shortest peaks for the  $S/N$  of truncated code.

### 6.1.2 With Data

The autocorrelation produces useful results only if an integration time of half the data duration is sufficient to produce enough gain to allow the detection of the trains of peaks. If the integration time is longer than half the data duration, periodic peak patterns are not formed and it is not possible to extract information from the autocorrelation. These statements are also valid for all cases of augmentation, truncation and cross-correlation.

### 6.2 Second Method: Cross-Correlation with the Original Code

The shift between the interleaved trains is equal to the length of the truncation or augmentation length divided by two. The total integration time for each peak is equal to the build-up time of each individual peak as the different peak trains are shifted relative of each other and the detection of the peaks is possible only if the S/N of the input signal is sufficiently good. The integration time has to be adjusted to allow the formation of two successive peaks from two successive trains.

### 6.3 Third Method: Cross-Correlation with a Test Code.

If the length of the modified code, either augmented or truncated, is known, a test code of the same length can be used to perform the cross-correlation. In that case, the shift between the successive trains of peaks is removed and it is possible to integrate as long as necessary to build up the required gain. It is a processing method particularly well suited to the processing of codes where the modified segments are short and represent a small percentage of the number of chips integrated during an integration period. In that case the loss of gain associated with the relatively short mismatch between the modified code and the test code can be neglected and the integration time can be set to allow peak detection given the S/N for the input signal. An extreme case is the cross-correlation of a modified code with 50% truncation with a test code whose initial fill is such that the wrong half of the code is used to perform the cross-correlation. No correlation peak results.

The special case of the cross-correlation of an augmented code with a test code having a different initial fill has to be mentioned. The energy in the correlation is then distributed among two peaks and, in the worst case, the two peaks have equal height. The integration time must be doubled to allow for the detection of the peaks.

#### 6.4 Fourth Method: Determination of the Initial Fill

##### 6.4.1 For an Augmented Code

The presence of the double-peak feature is an indication that the wrong initial fill is used. The correct initial fill can be determined by the following procedure. It is assumed that the length of the truncation is known and that the truncation is at the end of the code. The procedure consists of successively trying all possible initial fills, thus generating all the corresponding test codes. For each test code, the correlation is performed with the truncated code. The same segment of the modified code has to be used for all trials and the integration time should be the duration of the truncated code. The tallest correlation peak is associated with the use of the correct fill because all of the chips of the test code will then contribute to the peak.

##### 6.4.2 For a Truncated Code of the First Type

If the S/N is very good, it is conceptually possible to determine the initial fill and consequently which chips have been removed from the code, by applying the following procedure; this is similar to the method described in Section 4.3.2.

The procedure consists of successively trying all possible initial fills, thus generating all the corresponding test codes. It is assumed that the length of the truncation is known and that the truncation is at the end of the code. For each test code, the correlation is performed with the truncated code. The same segment of the modified code must be used for all trials and the integration time should be the total duration of the truncated code. The tallest correlation peak is associated with the use of the correct initial fill because in that case all of the chips of the test code contribute to the peak.

If the initial fill is incorrect, the test code will not start at the right location; thus, a few chips of the test code will not be identical to the given code and a smaller peak will be observed.

##### 6.4.3 For a Truncated Code of the Second Type

The comments of the preceding section also apply to the determination of the initial fill for a truncated code of the second type.

#### 7.0 ACKNOWLEDGEMENT

The author would like to thank Lt. S. Faulkner and Dr. D. Hill for many useful discussions about coding theory. The careful review of the manuscript made by Lt. Faulkner was very appreciated.

## 8.0 REFERENCES

- [1] M.W. Casseday, N.J. Berg, I.J. Abramovitz and J.N. Lee, 'Wide-Band Signal Processing Using the Two-Beam Surface Acoustic Wave Acoustooptic Time Integrating Correlator', IEEE Transactions on Sonic and Ultrasonics, vol.SU-28, no.3, May 1981, p.205-212.
- [2] C.S. Tsai, J.K. Wang and K.Y. Liao, 'Acousto-Optic Time-Integrating Correlators Using Integrated Optics Technology', SPIE vol.180, Real-Time Signal Processing II, 1979, p. 160-163.
- [3] W.T. Rhodes, 'Acousto-Optic Signal Processing: Convolution and Correlation', Proc. IEEE, vol.69, no.1, Jan 1981, p.65-79.
- [4] I.G. Fuss, 'Acoustooptic Signal Processor Based on a Mach-Zehnder Interferometer', Appl.Opt. vol.24, no.22. 15 Nov 1985, p.3866-3871.
- [5] D.A.B. Fogg, 'A Compact Bulk Acousto-Optic Time Integrating Correlator', Department of Defence of Australia, Technical Report ERL-0323-TR, Nov. 1984.
- [6] N. Brousseau and J.W.A. Salt, 'Design and Implementation of a Time-Integrating Correlator Using a Bulk Acousto-Optics Interaction', DREO TN 86-25.
- [7] A.P. Goutzoulis and B.V.K. Vijaya Kumar, 'Optimum Time-Integrating Acousto-Optic Correlator for Binary Codes', Optics Communications, vol.48, no.6, 15 Jan. 1984, p.393-397.
- [8] D. Casasent, A Goutzoulis and V.K. Vijaya Kumar, 'Time-Integrating Acoustooptic Correlator: Error Source Modelling', Appl. Opt., vol.23, no.18, 15 Sept 1984, p.3130-3137
- [9] J.B. Goodell, 'Optical Design Considerations for Acousto-Optic Systems', SPIE vol.936, Advances in Optical Information Processing III, 1988, p.22-28.
- [10] N.J. Berg and J.N. Lee, 'Acousto-Optic Signal Processing: Theory and Implementation', Marcel Dekker Inc. New York and Basel, 1983, p.291.
- [11] P. Kellman, 'Time-Integrating Optical Signal Processing', Ph.D. dissertation, Dept. of Electrical Engineering, Stanford University, June 1979.
- [12] A. Goutzoulis, D. Casasent and B.V.K. Vijaya Kumar, 'Detector Effects on Time-Integrating Correlator Performance', Appl. Opt., vol.24, no.8, 15 April 1985, p. 1224-1233.

- [13] R.A. Sprague and C.L. Koliopoulos, 'Time-Integrating Acoustooptic Correlator', Appl. Optics, vol.15, no.1, Jan 1976, p.89-92.
- [14] G. Silbershatz and D. Casasent, 'Hybrid Time and Space Integrating Processors for Spread Spectrum Applications', Appl. Opt., vol.22, no.14, 15 July 1983, p.2095-2103.
- [15] F.B. Rotz, 'Time-Integrating Optical Correlator', SPIE vol.202, Active Optical Devices, 1979, p.163-169.
- [16] H. Fukumasa, R. Kohno and H. Imai, 'Pseudo-Noise Sequences for Tracking and Data Relay Satellite and Related Systems", 1990 International Symposium on Information Theory and its Applications, HAWAII, U.S.A. Nov.27-30 1990, p.775-778.

## DOCUMENT CONTROL DATA

(Security classification of title, body of abstract and indexing annotation must be entered when the overall document is classified)

1. ORIGINATOR (the name and address of the organization preparing the document. Organizations for whom the document was prepared, e.g. Establishment sponsoring a contractor's report, or tasking agency, are entered in section 8.) NATIONAL DEFENCE DEFENCE RESEARCH ESTABLISHMENT OTTAWA SHIRLEY BAY, OTTAWA, ONTARIO K1A 0K2 CANADA		2. SECURITY CLASSIFICATION (overall security classification of the document including special warning terms if applicable)  UNCLASSIFIED	
3. TITLE (the complete document title as indicated on the title page. Its classification should be indicated by the appropriate abbreviation (S,C or U) in parentheses after the title.)  EFFECT OF CODE AUGMENTATION OR TRUNCATION ON THE SIGNALS PRODUCED BY A TIME-INTEGRATING CORRELATOR (U)			
4. AUTHORS (Last name, first name, middle initial) BROUSSEAU, N.			
5. DATE OF PUBLICATION (month and year of publication of document)  OCTOBER 1992	6a. NO. OF PAGES (total containing information. Include Annexes, Appendices, etc.) 77	6b. NO. OF REFS (total cited in document)  16	
7. DESCRIPTIVE NOTES (the category of the document, e.g. technical report, technical note or memorandum. If appropriate, enter the type of report, e.g. interim, progress, summary, annual or final. Give the inclusive dates when a specific reporting period is covered.)  DREO REPORT			
8. SPONSORING ACTIVITY (the name of the department project office or laboratory sponsoring the research and development. Include the address.) NATIONAL DEFENCE DEFENCE RESEARCH ESTABLISHMENT OTTAWA SHIRLEY BAY, OTTAWA, ONTARIO K1A 0K2 CANADA			
9a. PROJECT OR GRANT NO. (if appropriate, the applicable research and development project or grant number under which the document was written. Please specify whether project or grant)  041LQ		9b. CONTRACT NO. (if appropriate, the applicable number under which the document was written)	
10a. ORIGINATOR'S DOCUMENT NUMBER (the official document number by which the document is identified by the originating activity. This number must be unique to this document.)  DREO TECHNICAL NOTE 92-11		10b. OTHER DOCUMENT NOS. (Any other numbers which may be assigned this document either by the originator or by the sponsor)	
11. DOCUMENT AVAILABILITY (any limitations on further dissemination of the document, other than those imposed by security classification) <input checked="" type="checkbox"/> (X) Unlimited distribution <input type="checkbox"/> ( ) Distribution limited to defence departments and defence contractors; further distribution only as approved <input type="checkbox"/> ( ) Distribution limited to defence departments and Canadian defence contractors; further distribution only as approved <input type="checkbox"/> ( ) Distribution limited to government departments and agencies; further distribution only as approved <input type="checkbox"/> ( ) Distribution limited to defence departments; further distribution only as approved <input type="checkbox"/> ( ) Other (please specify):			
12. DOCUMENT ANNOUNCEMENT (any limitation to the bibliographic announcement of this document. This will normally correspond to the Document Availability (11). However, where further distribution (beyond the audience specified in 11) is possible, a wider announcement audience may be selected.)			

## SECURITY CLASSIFICATION OF FORM

13. **ABSTRACT** ( a brief and factual summary of the document. It may also appear elsewhere in the body of the document itself. It is highly desirable that the abstract of classified documents be unclassified. Each paragraph of the abstract shall begin with an indication of the security classification of the information in the paragraph (unless the document itself is unclassified) represented as (S), (C), or (U). It is not necessary to include here abstracts in both official languages unless the text is bilingual).

(U) The purpose of this study is to analyse the characteristics of the signals produced by a time-integrating correlator when processing augmented or truncated codes. It deals specifically with the description of the peak trains generated by either the autocorrelation of the modified code, the cross-correlation of the modified code with the original code or the cross-correlation of the modified code with a test code of the same length. It is demonstrated that the complex peak patterns thus generated contain information about the modification of the code and that it is possible to retrieve that information by applying specific processing methods. Four processing methods are proposed. The first method extracts information from the peak patterns generated by the autocorrelation of the modified signal. The second method uses the cross-correlation of the modified signal with the original signal while the third method deals with the cross-correlation of the modified code with a test code that has the same length as the modified code. The fourth method allows the determination of the initial fill of truncated codes when the signal-to-noise ratio is sufficiently good.

14. **KEYWORDS, DESCRIPTORS or IDENTIFIERS** (technically meaningful terms or short phrases that characterize a document and could be helpful in cataloguing the document. They should be selected so that no security classification is required. Identifiers, such as equipment model designation, trade name, military project code name, geographic location may also be included. If possible keywords should be selected from a published thesaurus. e.g. Thesaurus of Engineering and Scientific Terms (TEST) and that thesaurus-identified. If it is not possible to select indexing terms which are Unclassified, the classification of each should be indicated as with the title.)

TIME-INTEGRATING CORRELATOR  
OPTICAL CORRELATION  
AUGMENTED CODES  
TRUNCATED CODES